Lithological and Geomorphological Indicators of Glacial Genesis in the Upper Quaternary Strata, Nadym River Basin

Oleg Sizov[1], Anna Volvakh[2], Molodkov A.N.[3], Andrey Vishnevskiy[4], Andrey Soromotin[5], and Evgeny Abakumov[6]

[1]Oil and Gas Research Institute, Russian Academy of Sciences, Moscow, Russia

[2]Sobolev Institute of Geology and Mineralogy, Siberian Branch of Russian Academy of Sciences, Novosibirsk, Russia

[3] Tallinn University of Technology, Tallinn

[4]Novosibirsk State University, Novosibirsk, Russia

[5]Tyumen State University, Tyumen, Russia

[6]Saint-Petersburg State University, Saint Petersburg, Russia

Abstract

Analyzing the genesis of Quaternary sediments is important for understanding the glaciation history and development of marine sediments in the northern part of the Western Siberia. The problem is relevant since there is no consistent concept of the Quaternary sediments genesis in the north of Western Siberia. Their formation is associated with marine, glacial and interglacial sedimentation conditions. The research objective is to identify the persistent features characterizing the conditions of sedimentation and relief formation using the Nadym river basin as an example. The best method for studying this problem is a comprehensive analysis of the lithological, chronostratigraphic, petrographic and geomorphological studies of the Quaternary sediments upper strata. This study provides data from the analysis of the basic characteristics of quartz grains at the site. The rounding and morphology of the quartz grains provide evidence of possible glacial processing of some of the site strata. A petrographic study of selected boulder samples was performed. Some of them, by the shape and presence of striation, can be attributed to ice basins. The first use of a detailed digital elevation model applied to the study area made it possible to identify specific relief forms that could very likely be created during glaciations. Based on the analysis, we propose to consider the vast lake-alluvial plains in the Nadym river basin as periglacial regions. This idea lays the lithological framework for understanding the reasons for the formation of the modern landscape structure. The materials and descriptions provided are of interest to researchers of Quaternary sediments, topography, vegetation, and soil cover; particularly researchers engaged in revising the history of the natural environment development in the north of Western Siberia.

Keywords: Western Siberia, paleogeography, cover glaciation, Quaternary deposits, quartz grains, petrography, DEM

Introduction

The history of geomorphological development in the northern part of Western Siberia was a subject of intensive discussion at the end of the 20th century. The stratigraphy of the Yenisey river estuary is a key factor of the West-Siberian lowland quaternary evolution. Numerous examples of sedimentation alternation induced by various cover glaciations of different ages and thicknesses are presented. This series of sediments was used as a background for geological interpretation of the history of Western-Siberian lowland. The Q-43 national geological map of Russia for this region indicates the dominance of glacial and fluvioglacial types of the surface sediments (Alyavdin and Mokin, 1957) The possible existence of ice sheets and related permafrost sediments was identified as a key issue at the beginning of the

systematic geological study of the north of West Siberia in the 1960s. Some researchers (e.g., Svendsen et al., 2004) suggested that there were extensive glaciations that resulted in blocking the Yenisei, Pur, Taz, Nadym rivers at certain stages, leading to the formation of large glacier dammed lakes (Grosvald, 1999)

Another point of view considers possible glaciation on the plain (e.g., Generalov, 1986). It explains why the landforms are a sequence of terraces formed by marine transgressions of various ages. There is also an opinion that the glaciation was localized in the form of ice caps on separate watersheds and that the river flows of the Ob, Yenisei, and other rivers were unblocked (Velichko, 1987; Velichko et al., 1997) Bolshiyanov (2006) challenged this opinion and introduced the "passive glaciation" concept. In this context, it is assumed that the sea level fluctuations might have created extensive abrasion platforms. Another viewpoint suggests that the forms of relief which previously were considered as glacial and fluvioglacial (moraines and eskers), did not originate from cover glaciations, but resulted from erosion, abrasion, and thermokarst outcrops associated with permafrost-erosion and tectonic processes of the late Pleistocene. It was suggested that isolated parts of Smarovskoye glaciation (MIS8, 300,000 to 230,000 years ago) existed in some areas of the Tyumen region combined with relics of ancient marine terraces (Lazukov, 1972). Later, there was a heated discussion in the Russian geology community regarding the nature of possible glaciations and sedimentation history of Western Siberia. It was suggested that glaciations extended up to Siberian ridges that continued as the ancient periglacial Mansyiskoye lake (Grosvald, 1999). Bolshiyanov (2006) suggested that the glaciations were passive, without forming a discontinuous cover or preferential flow blocking in the area topography. At the same time, the abrasion relief with extended ledges was formed in the late Pleistocene period. Finally, the Q-42-43 national geological map indicates that there is a combination of both terrestrial glacial and marine glacial sediments and numerous lake terraces in Western Siberia. Nowadays, the glacial sediments are excluded from the current version of the national geological map (Babushkin, 1995) which contradicts the results obtained by Astakhov et al. (2016) and Fredin et al. (2012). Currently, there is no uniform concept of the landforms genesis in Western Siberia. The basing of the Nadym River is considered as most important for the Quaternary interpretation of the local Pleistocene history. The topography and sediments of the Nadym River provide the most information for the study of glacial landforms. Many field investigations and remote sensing operations were completed by multiple generations of researchers, providing a valuable baseline for future studies. The results of studying the Nadym River and adjacent areas, combined with other data, served as a basis for a classification of the Quaternary deposits in West Siberia (Maslennikov, 1998; Sedov et al, 2016; Sheinkman et al, 2016; Rusakov et al, 2018). Nevertheless, the current geological map (Faibusovic and Abakumova, 2015) still has unsolved issues that are highlighted as new geological and geomorphological data are obtained.

The study objective is to summarize the results of detailed lithological, chronostragraphic, petrographic and geomorphological studies conducted in the

Nadym River basin, and to identify the origins of the key factors of sedimentation accumulation and topography.

Materials and Methods

Fieldwork was conducted in 2016-2018 in the Nadym River Basin, including the valleys of its main tributaries: Kheygiyaha, Yarudey, Tanlova, Left and Right Khetta. The region is characterized by a moderate human-induced burden. There are main gas pipelines (Urengoy-Pomara-Uzhhorod, Nadym-Punga-Lower Tura, etc.), high-voltage power transmission lines (200, 500 kV), an oil pipeline Yarudeyskoe field CGS to Puryel OPS), and the Nadym-Yagelskoye asphalt road. The survey covered the natural exposures along riverbanks, walls of dry quarries located at the watersheds and river terraces as the most informative terrain features. This paper is based on the results of detailed studies of the five most prominent stratigraphy sections of the upper part of Quaternary sediments (Fig. 1). B Table 1 For clarity, the section coordinates, their locations, suevey dates and the total thickness of the studied deposits are specified.

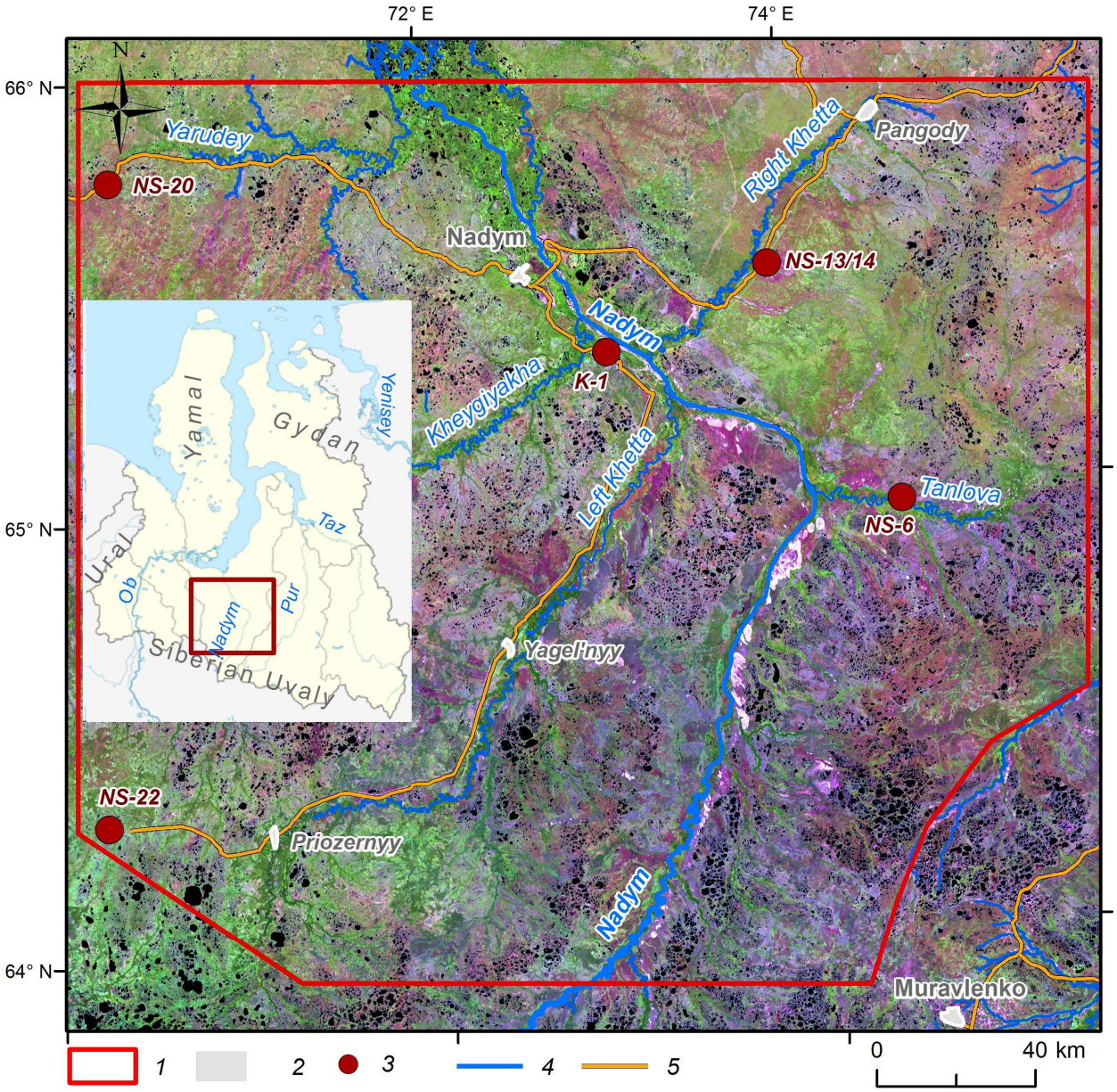

Fig. 1. Overview map: 1: study area; 2: settlements; 3: studied and sampled locations; 4: waterways; 5: roads. Background image: Landsat 8, 2000.

Table 1
Site Properties

N	Coordinates N, E	Top of sectrion elevation, m a.s.l.	Geogenic location	Sampling point location	Survey date	Thickness, m
K-1	65.351044 72.974041	24	Second above flood plain terrace	Wall of quarry	21.08.2016	4.2
NS-6	64.974808 74.499714	44	Second above flood plain terrace	River break	18.08.2017	9.5
NS - 13/14	65.52992 73.875985	44,5	Kamiform hill	Top and slope of hill	22.08.2017	5.1

NS-20	65.778072 70.29182	57	Easker sediments	Wall of quarry	11.08.2018	16
NS-22	64.31688 70.232456	130	Watershed	Wall of quarry	13.08.2018	1.5

Samples for bulk chemical composition, grain size distribution, sand quartz grain morphoscopy and morphometry, as well as luminescent analysis of sandy textured particles of feldspars were taken from each specified layer of the studied sections in order to clarify the conditions of the sediment formation.

The bulk content of oxides was determined by the X-ray fluorescence method at the Analytical Center for Multi-Elemental and Isotope Research, Siberian Branch (SB), Russian Academy of Sciences (RAS), Novosibirsk, Russia, and at the laboratory of the Institute for Physical, Chemical and Biological Problems of Soil Science (Pushchino, Russia). The grain size distribution was determined by conventional fractions separation (sieve analysis) of samples with the Fritsch Analysette 3 vibratory sieve shaker. The fractions were weighed with laboratory scales, 0.1 g accuracy. 17 samples from the sections NS-6 and NS-13/14 were analyzed at the Laboratory of Ground Mechanics, Institute of Cryosphere of the Earth, Tyumen Research Center with the Mastersizer 3000E laser diffraction particle size analyzer (Malvern Panalytical, Britain). Since different laboratories measured the granulometric composition, the figures for the lightest fractions are slightly different.

The Altami CM0870-T binocular microscope was used to study the quartz grains (50 grains per sample) taken from the coarse sand fraction. The grain surface morphology was studied with the JEOL JSM-6510LV scanning electron microscope (SEM) using the secondary electron image (SEI) at the Analytical Center for Multi-Elemental and Isotope Research, SB, RAS. According to the technique applied (Velichko and Timireva, 1995), the grain scale was determined using Rukhin (1969, Fig. 2) and Khabakov (1946), where 0 is an angular, and IV is a perfectly rounded grain. The coefficients of roundness and the grades of dullness (Velichko and Timireva, 1995) were estimated for each sample. The dullness of the grains was determined visually as glossy (shiny), quarter-matte, half-matte, and matte. The grain surface microrelief structure study was based on numerous published diagnostic features found in grains with various genesis and sediment accumulation conditions (e.g. Velichko and Timireva, 1995; Krinsley, Doornkamp, 2011; Vos et al., 2014; Woronko, 2016; Kalinska-Nartisa et al., 2017). The previous studies in Western Siberia that examined sand quartz grain micromorphology covered peat histic sand deposits in the area of Siberian Uvals, valleys of the rivers Taz and Pur, (Velichko et al., 2011) and aeolian sediments of the southern part of Western Siberia (e.g. Sizikova, Zykina, 2015).

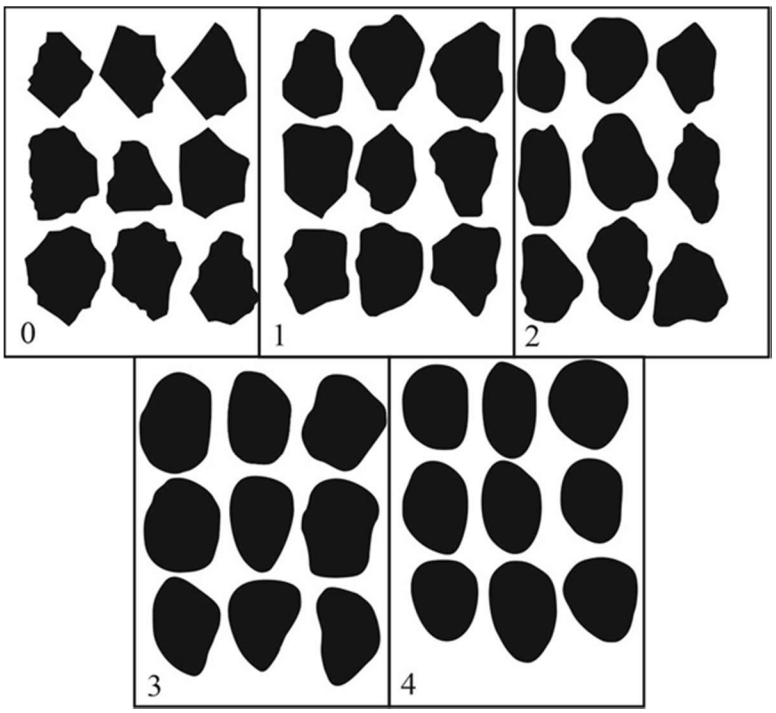

Fig. 2. Pattern (Rukhin, 1969)
0, 1, 2, 3, 4 are the classes of roundness (Khabakov, 1946)

The potassium feldspar-based infrared optically-stimulated luminescence (IR-OSL) dating method was applied to produce an absolute chronology of the deposits from the five sections studied in the present work. The upper limit of the method is normally 300–500 ka, depending on burial conditions and the physical properties of the mineral. The reliability of the dating technique used in the present study is demonstrated by comparative results obtained using several numerical dating methods (mollusc shell-based electron spin resonance (ESR), quartz-based optically stimulated afterglow (OSA), U-Th, 14C) applied to the same sedimentary samples (Molodkov, 2012). An overview of the IR-OSL dating procedure is presented by Molodkov and Bitinas (2006.) All IR-OSL ages reported in this paper were obtained in the Research Laboratory for Quaternary Geochronology, Institute of Geology, Tallinn University of Technology.

In addition to the analysis at the sampling area, samples were taken for petrographic examination. The samples were cut perpendicular to the bedding direction (if any) and made into transparent sections. The Carl Zeiss AxioScope A1 optical microscope at the Geology and Mineralogy Institute, SB RAS (Novosibirsk) was used.

For the first time for the studied area, digital terrain models (DTM) with spatial resolution of 12 and 26 m/px based on TerraSAR -X and TanDEM -X radar data were used to characterize the geomorphological structure. The mapping is based on the remote features available in the literature (Atkinson et al., 2014; Astakhov et al., 2016, etc.) and the comparison of the field and remote sensing data (Table 2).

Table 2

Remotedly sensed features of glacial and fluvioglacial relief

Relief features	Remotedly sensed features
Kame-like hummocks	Irregularly scattered hills and ridges with their relative elevation not exceeding 10-20 m (Fig. 2). The hills have plateau-like summit, the slopes are gently convex, the slopness varies. The hills and ridges are easily identified on the DTM agaist the flattened background; often they are separated by no-outflow basins and hollows. The hills are at the highest parts of the watersheds and often from groups or even curved chains oriented NE to SW, or E to W. Sparse vegetation areas are associated with the highest parts of the hills.
End moraines	Mostly associated with the watersheds. They are narrow, tortuous upheavals (relative elevation is up to 5-7 m, sometimes to 10 m.) The survival rate varies. They van be in the form of high linear upheavals with steep clopes to low kettelbacks 10-12 km long. With high resolution DTMs (2-10 m), the small local boaundary moraine formations are easily identified; for mid-resolution DTMs (25-30 m) the large features with a low survival rate are identified. The key properties are the length and the position: the flat moraine pattern usually forms an interconnected structure that reflects the ice sheet extents and the stages of its degradation.
Parallel ridges	As opposed to the terminal moraine ridges, the linear ridges are smaller and shorter while their direction is more pronounced (almost no bends.) When ridges are poorly expressed, an additional indicator is a linear structure of the multispectral image caused by the similar orientation of the river valleys, chains of small lakes, forest and bog boundaries..
Valley trains	Twisted similarly to smooth river meanders. Nowadays they are swamped and turned into lakes. Merging and splitting, they form a typical pattern of the hydrographic network.. The valleys are often associated with expected drainwater sources mostly located in glacial accumulative formations on the watersheds. The valleys often terminate with chains of lakes perfectly visible in satellite images.

In addition, public multi-spectrum space images from Sentinel-2 (10 m/px.) were used to clarify the location of such natural features as rivers, lakes, swamps, and forests (https://scihub.copernicus.eu/.)

3. Results

3.1. Characteristics of the Sections

The summary results of the Quaternary sediment section study are shown in Figs 3-7 and Annexes 1, 2. From the data obtained, the following characteristic conditions of sediment accumulation can be distinguished:

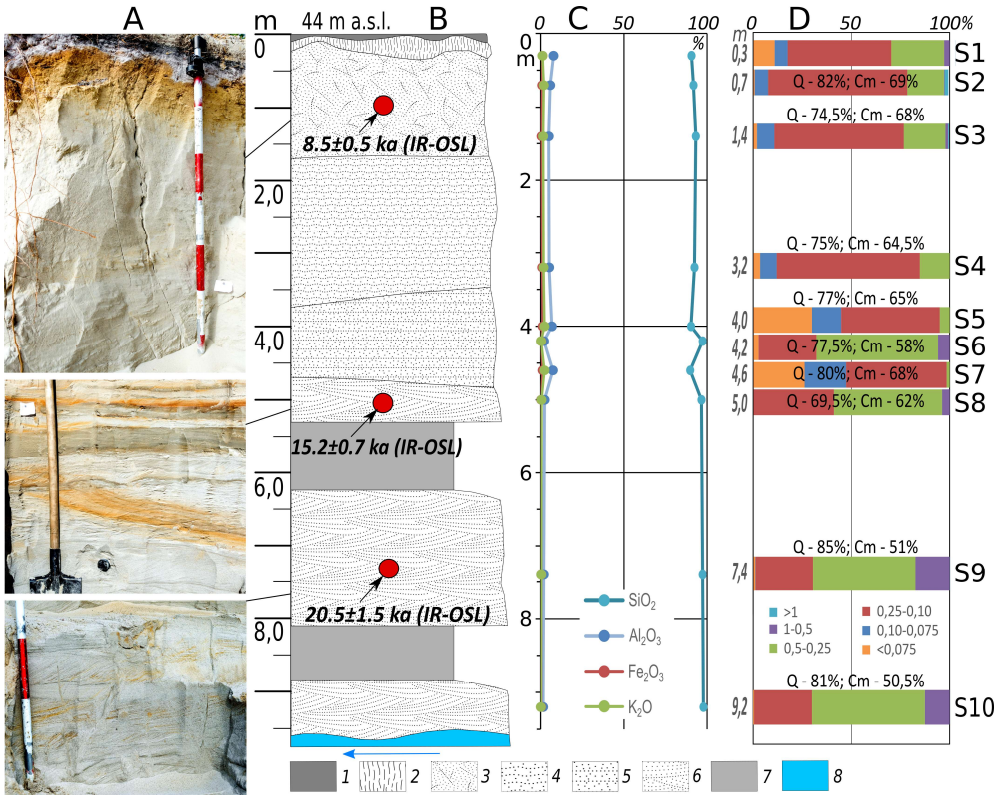

Fig. 3. Summary results of research for NS-6 section. A: photographs (by Sizov in 2017); B: geological structure and the dating results (refer to Table 3); C: bulk chemical data; D: grain size distribution (fractions, mm) Symbols: 1: podzol horizon of modern soil; 2: illivial-iron (spodic) horizon of modern soil; 3: sands without stratification; 4: undulating sand with secondary ironing; 5: horizontally layered sand with stratification of loam; 6: medium-and coarse-grained oblique sand; 7: colluvium; 8: river level; Q: coefficient of roundness of the sand quartz grains; Cm: degree of dullness; S: sample number.

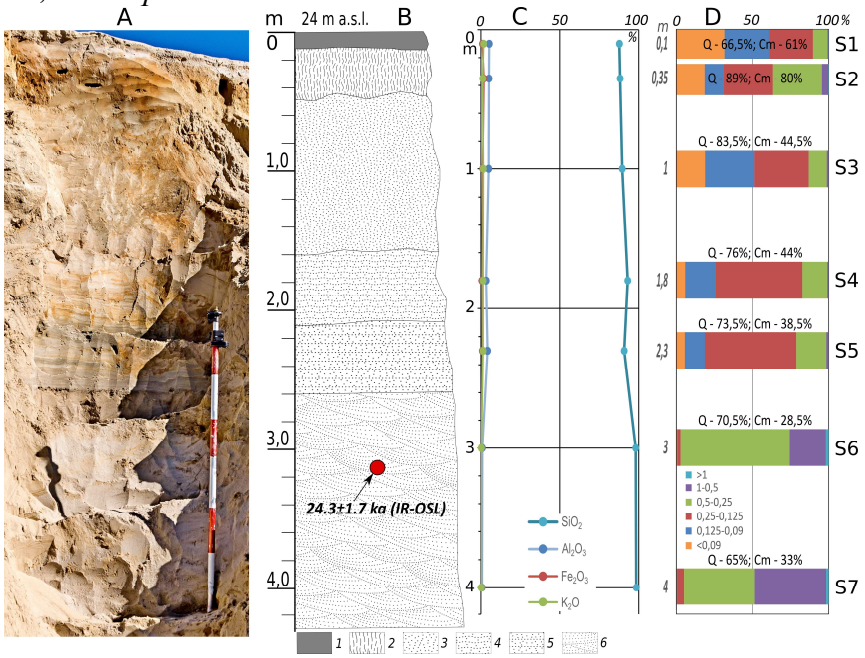

Fig. 4. Summary results of research for K-1 section: A: photographs (by Sizov in 2016); B: geological structure and the dating results (refer to Table 3); C: bulk chemical data; D: grain size distribution (fractions, mm) Symbols: 1: podzol horizon of modern soil; 2: illivial-iron (spodic) horizon of modern soil; 3: sands without stratification; 4: undulating sand with secondary ironing; 5: horizontally layered sand with stratification of loam; 6: medium-and coarse-grained oblique sand; 7: colluvium; 8: river level; Q: coefficient of roundness of the sand

quartz grains; Cm: degree of dullness;
S: sample number.

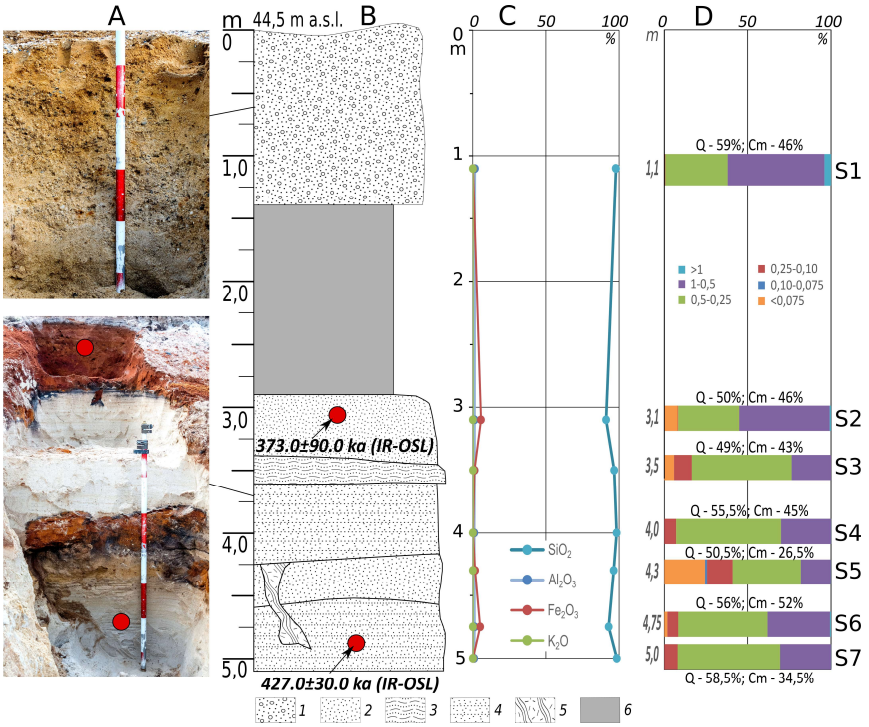

Fig. 5. Summary results of research for NS-13/14 section: A: photographs (by Sizov in 2017); B: geological structure and the dating results (refer to Table 32); C: bulk chemical data; D: grain size distribution (fractions, mm) Symbols: 1: coarse sand with pebbles; 2: unstratified red sand; 3: undulating black sand; 4: horizontally layered sand; 5: wedge filled by deposits of the overlying layer ~~Layer 4~~; 6: colluviums; Q: coefficient of roundness of the sand quartz grain; Cm: degree of dullness; S: sample number.

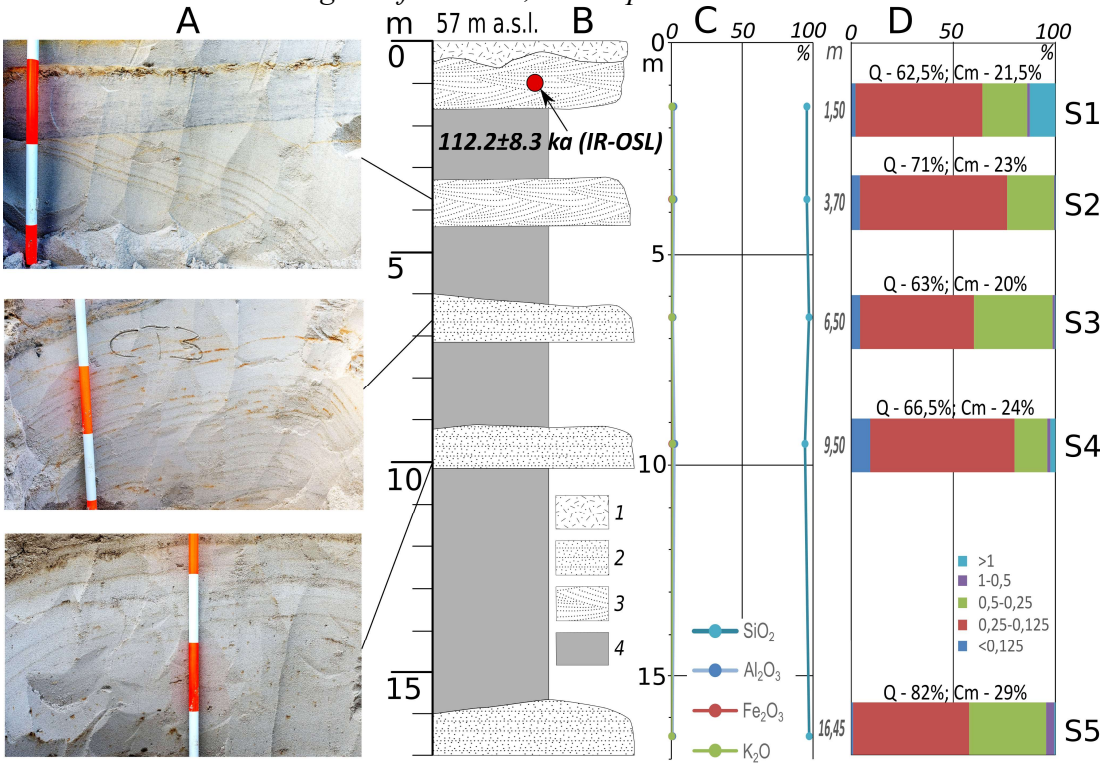

Fig. 6. Summary results of research for section NS-20: A: photographs (by Sizov in 2018); B: geological structure and the dating results (refer to Table 3); C: bulk chemical data; D: grain size distribution (fractions, mm) Symbols: 1: overburden; 2: horizontally layered sand;

3: medium-and coarse-grained oblique sand; 4: colluvium; Q: coefficient of roundness of the sand quartz grains; Cm: degree of dullness; S: sample number.

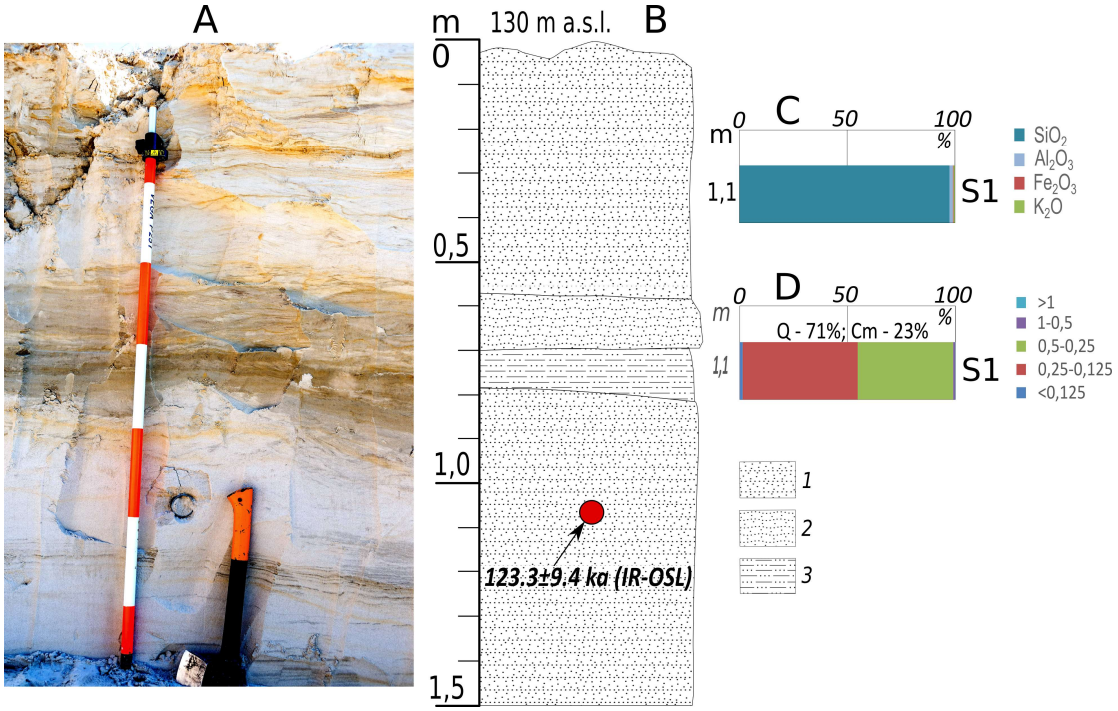

Fig. 7. Summary results of research for section NS-22: A: photographs (by Sizov in 2018); B: geological structure and the dating results (refer to Table 3); C: bulk chemical data; D: grain size distribution (fractions, mm) Symbols: 1: horizontally layered grey sand; 2: oblique layered sand; 3: horizontally layered sandy loam; Q: coefficient of roundness of the sand quartz grain; Cm: degree of dullness; S: sample number.

1. Alluvial deposits predominate at the lower geomorphological level (up to 40-45 m) Sections K-1 and NS-6 show the similar structure of the second above-ground terrace of the Nadym and Tanlov rivers: in the upper part, thick podzolized soil is formed over the aeolian deposits in the middle part, floodplain type deposits dominate and in the lower part they are replaced by well-leached gray layered sand. Down the profile, the SiO_2 content increases, while the content of other chemical elements is low. The middle part of the section is dominated by fine and medium-grained sand, the portion of large fractions increases in the lower part where single pebbles up to 3-4 cm are found. There are no permafrost-affected sediments.

2. At the middle level, the sections show the structure of a NS-13/14 kamiform hill and a linear-oriented relief (NS-20). The top of the hill is covered with a solid layer of pebbles; at 1.2 m depth, it is followed by coarse sand. Sandy deposits forming two distinct cycles are exposed in the middle part of the hill. The unbroken red-colored sand is followed by black sand with slightly horizontal orientation, which in turn is followed by light-grayish horizontally layered sand. In the lower profile, the cycle is repeated; the difference is that the layer of intensively reddish sand is not as thick. In the left lower part of the section, there is a frost wedge microdepression, filled with the overlying layer sediments. In general, the section is dominated by medium- and coarse-grained sands of monomineral composition (the shares of Fe, Al and other chemical elements are insignificant)

In section NS-20, the slope of the extended elevation is exposed. It is composed of a monotonic body of grey monomineral parallel and oblique-oriented quartz sand. The sands throughout the section have an identical grey color and fine-grained composition. The presence of thin iron-containing layers does not affect the chemical composition of sediments: SiO_2 prevails in all layers. Local hills up to 5-8 m high covered with large pebbles and boulders on the surface were found on the top of the ridge along the survey path. In an exploration ditch on the top of the microhill (1.5 m deep), large-grained, non-laminated sandy sediment with the abundance of angular pebbles, gravel, and single large (up to 30-40 cm) boulders were exposed. Their structure is similar to the deposits of the upper part of section NS-13/14. In sections, permafrost sediments traces of frost cracking.

3. The NS-22 is at the upper watershed in a small quarry. The qyarry exposes sandy and sandy-loam bedded deposits of the large hill. Sands in the sample are grey-colored, fine and medium-grained. The SiO_2 content is 96.49%. A huge number of large, weakly rounded boulders, up to 1.5 m in size, was found in the quarry and on the sandbank of the nearest lake (100-200 m from the quarry.)

It should be noted that grey fine, medium- and coarse-grained sands of monomineral quart composition are present in all sections (except for NS-13/14). In river terraces, such sands have oblique lamination, while on the watershed they are oriented horizontally. The sands have no permafrost features, cracking traces and, in general, poor chemical composition. A landscape vegetation feature of such sediments is pine sparse forests, which are able to grow on poor sandy soils with a well-drained hydrologic behavior. Sandy soils lack organic materials and debris of fossil clams, and do not show any salt content. Despite the presence of large debris on the scree slopes; boulders do not occur directly in the sands. Based on morphological, particle size and chemical features infer we that this type of sand sediment could be formed in subaquatic conditions in more severe environments as compared to modern climatic conditions.

3.2. Sediments Dating Results

IR-OSL ages for the sediment samples from the sites studied and the related analytical data are listed in Table 3.

Table 3

Absolute dating by the IR-OSL method

Section	Sampling depth	Sample code	Age	U (ppm)	Th (ppm)	K (%)
K	3.15	RLQG 2443-057	24.3 ± 1.7	0.11	0.45	0.01
NS-6	1.0	RLQG 2563-019	8.5 ± 0.5	0.79	0.73	0.94
NS-6	5.0	RLQG 2564-118	15.2 ± 0.7	0.01	0.00	0.14
NS-6	7.3	RLQG 2565-118	20.5 ±1.5	0.01	0.00	0.14
NS-13/14	3.1	RLQG 2567-019	373.0 ± 90.0	0.00	0.00	0.00
NS-13/14	4.9	RLQG 2568-019	427.0 ± 30.0	0.35	0.74	0.00
NS-20	1.1	RLQG 2577-059	112.2 ± 8.3	0.96	4.19	0.34
NS-22	1.0	RLQG 2578-059	123.3 ± 9.4	1.29	2.00	1.31

From section K, a single date of 24.3±1.7 (RLQG 2443-057) was obtained at the depth of 3.2 m. According to this age, its formation took place at the very end of the third (Lipovka-Novoselovo) warm phase, which was recorded in the north of Western Siberia during MIS 3 (Marine Isotope Stage 3) by both the ^{14}C (Kind, 1974) and clam shell-based ESR (Molodkov, 2020) methods.

The normal sequence of the youngest ages of 20.5 ka (RLQG 2565-118), 15.2 ka (RLQG 2564-118), and 8.5 ka (RLQG 2563-019) was obtained for section NS-6 at the depths of 7.3 m, 5.0 m, and 1.0 m, respectively. Specific analytical features suggest the supply of the sedimentary rock from the same source area. The genesis of the deposits is also identical. It implies similar conditions for the rock transfer despite the likely difference in climatic conditions.

Somewhat unexpected were the dating results for two consecutive layers in section NS-13/14: 427.0 ka (RLQG2568-019) and 373.0 ka (RLQG2567-019) Finding very old Pleistocene deposits (MIS 11) is exceedingly rare. Judging from the analytics, the sedimentary rock in these layers came from different source areas and has fluvial, most likely river genesis. Under the given conditions of burial and physical properties of the mineral, the upper dating limit may be at least three times higher (i.e., up to about a million years)

The last two datings at 123.3 ka (RLQG 2578-059) and 112.2 ka (RLQG 2577-059) were obtained from two sections: NS-22 and NS-20, respectively. Their common feature is that both of them fall into MIS 5, as well as the fact that the corresponding sedimentary rock also came from various source areas. The studied sediments on the base of a group of key features are supposed to have fluvial (river and lake) origin.

3.3. Sand Quartz Grain Morphoscopy and Morphometry.

Refer to Annexes 4-13 for the key results: coefficient of roundnesss, degrees of dullness, and examples of the quartz grain appearance. The following is a brief description of the main features.

NS-6. Aeolian genetic group. The upper part of the section (samples S2 and S3) is characterized by a high coefficient of roundnesss (Q; 74.5 - 82%) and degree of matting (Cm; 68 - 69%) IV^{th} rounding class matte grains prevail; the complete grain distribution vs. rounding and surface dullness are shown in Annex 4. The most common element of grains microrelief in the S1 sample is a micro-pitted surface (Annex 9 a, b), which is a feature of aeolian transportation (Velichko and Timireva, 1995). Chemical etching is sometimes found in depressions. High coefficients of roundness (Q) and degrees of dullness (Cm) along with the predominance of micro-pitted grain texture suggest the dominance of aeolian processes during the sedimentation. Several grains show signs of subaquatic treatment and origin in the form of crescentic depressions and V-shapes percussions (Annexes 9 a, b), which preceded the aeolian stage. It seems to be associated with the accumulation of rock from the river valleys.

For quartz grains from the floodplain deposits (samples S4-S8), the rounding coefficient (Q) is within the range of 65-80%; the degree of dullness (Cm) is 58-68% (Fig. 3). On average, IV rounding class grains (Refer to Annex 4) with a half-

matte surface prevail in the samples. The number of completely glossy grains increases (up to 22%) The entire grain surfaces have signs of subaquatic processing: V-shaped percussions (Annex 9 d), often forming a fine-pitted surface (Annex 9 c, d), and separate crescent gouges. Many grains show traces of aeolian treatment, expressed as a micro-pitted texture (Annex 9 c), which corresponds well to a sufficiently large share of matte grains in the sample. It can be assumed that deposits of this layer are formed by fluvial river and aeolian processes in the coastal environment.

For samples from the lower part of the section (samples S9, S10) Q = 81-85% and Cm is 50.5-51%. Most grains belong to the IV rounding class. The number of glossy grains (up to 32%) is significantly higher than in overlying sediments (Annex 4) The primary grain treatment traces on the surface of all grains, regardless of the roundness and dullness, are fine-pitted surfaces (Annex 9 e, f) and individual well-developed V-shaped microdepressions (Annex 9 f), which is a sign of active river fluvial transportation. There are grains of the II and III classes of roundness; they differ from most grains by the presence of flat faces (Annex 9 g, h). The shapes of these grains resulted from the previous stages of grain treatment. There are also signs of aqua treatment on its surfaces (Annex 9 g, h).The K-1 grain distribution across the section matches well the morphometric and morphological properties of the NS-6 section. Refer to Annex5 for the grain distribution by roundness and stroe. Layer 6 (samples S6-S7) lying in the base of the section provides important information. These samples differ in grain morphology from overlying sediments. They are characterized by the lowest cross-sectional values of the coefficient of roundness (63-65%) and the degree of matting (33-35%), the presence of glossy grains in all classes of roundness (Annex 10), constrained or ground flat faces at grains, and the development of sickle-like texture and fine pits on the grain surface. With these features, it can be concluded that this layer was formed by fluvial processes, but it should be emphasized that there is a rock in its composition that may have been exposed to glacial processes in the past.

NS-13/14. For S1 deposits Q= 59% and Cm = 46%. Angular grains, class I (32%) and medium-rounded grains, class II (24%) predominate. Most grains have half-matte (34%) and quarter-matte (32%) surface (Annex 6) The grains can be categorized into two groups. The first group is represented by well-rounded mature grains with a ubiquitous fine-pitted surface (Annex 11 a), which is a sign of treatment by aqueous streams. In the second group, there are grains of irregular shape (Annex 11 b), often with multiple or conchoidal fractures. The faces have traces of treatment in subaquatic environment. Grains of the second group show separate V-shaped and rarely crescentic-shaped percussions; their number and location indicate a lower exposure to water flow. The presence of these two different groups of grains suggests the ingress of rock from different sources of the rock. One one them could be the subangular fluvioglacial deposits.

For underlying deposits (S2-S7) Q=49 – 58.5% and Cm=26.5-52%. There, poorly-rounded and middle-rounded grains of classes I and II with a glossy or quarter-matte surface prevail (Annex 6). The grain surface is dominated by traces of low-activity subaquatic treatment: V-shaped and crescentic microdepressions

(Annex 11 c-h). Irregular grains with smooth surfaces are most common, often with fractures (Annex 11 e, f, h), which probably indicates its arrival from a source with poorly rounded materials. There are grains with conchoidal fractures formed by desquamation processes due to grain freezing (Velichko and Timireva, 1995) or under a big pressure applied to the grain (Immonen et al., 2014; Vos et al., 2014.) There are also V-shaped percussions along its surface, suggesting that the deformation occurred before the last fluvial treatment. Many grains were highly exposed to chemical processes expressed as etching through the depressions on the grain and the Fe-Mn skins. The development of V-shaped forms only along the protruding parts of the grain, a well-developed crescentic-shaped texture and non-ubiquitous fine-pits, the average values of the coefficient of roundness and low degrees of maturation suggest that the final processing of grains occurred in a relatively calm aquatic environment. For S2 and S3 samples, in addition to traces of subaquatic treatment, there are grains with small micro-pits (Annex 11 c, d), a sign of aeolian treatment of grains.

NS-20. For samples S1-S5, the coefficient of roundness (Q) is in the range of 62.5-82% and the degree of dullness (Cm) is 20-29%. Glossy grains of II and III classes of roundness prevail (Annex 7). In the most sediments (S1), there are signs of aeolian treatment of grains expressed as micro-pits (Annex 12 a, b). However, they have a rather low value of Cm, which is not typical of aeolian deposits. This suggests that the local aeolian redeposition of underlying sediments occurred. The underlying layers (S2-S5) have sediment features; their formation is probably associated with fluvioglacial processes: the surface of most grains is highly uneven, cavernous, and strongly mechanically deformed. These properties can be found in glacial conditions (at the stages of previous processing.) This is also suggested by the presence of deep-pits, grooves and parallel scratches of various configurations (Annex 12 c, d, h). The last agent in their treatment was a subaquatic process, as indicated by frequently occurring V-shaped and crescentic depressions (Annex 12 e, f, g).

NS-22. The coefficient of roundness (Q) is 79% and the degree of dullness (Cm) is 31%. Most of the grains belong to class III of roundness, a slightly smaller number of grains are of class IV; glossy grains prevail (Annex 8). The morphology of the grain surface is quite uniform and is mainly represented by grains with fine pits covering the grain surface almost completely (Annex 13 a-f) or developed only on microelevation parts of the grain (Annex 13 e, f). This surface is a characteristic feature of the long-term grain processing in a sufficiently active subaquatic environment.

3.4. Petrography

The petrographic analysis of 15 samples taken in a quarry nearby the section AS-3 (fig. 8, coordinates: N65.061417°, E72.943848°) enabled to distinguish several groups of materials:

1) The first group (6 samples) is presented by grey, yellowish-grey, and greenish-grey fine-grained and very fine-grained sandstone and siltstone with slab jointing. They are usually moderately or poorly sorted and have primary foliation

that is emphasized by the regular orientation of flattened grains, varying grain size, and matrix content. The matrix is hydromicaceous clay, sometimes with ferruginous cement, with a small portion of silica. The fragments are usually sub-rounded or sub-angular. The rock is composed of polymictic sandstones, similar to arkoses sandstones. Quartz and feldspar prevail among the mineral grains, composing ~30 vol% of the fragments, while another third is predominantly composed of siliceous rock fragments. Some samples contain significant amounts of muscovite (up to 5% by volume), chlorite (including pseudomorphs after the dark-colored minerals), and epidote. The presence of muscovite could be an indicator of low weathering of initial sediments.

2) Pebbles and boulders of the second group of quarzitic and quartz sandstone (6 samples) feature angular forms. The textures are usually massive and vary from poorly to well sorted. The cement is predominantly quartz or quartz-hydromicaceous, sometimes with goethite. The grain size varies greatly, but medium-sized varieties prevail. More than 95% of grains are quartz and siliceous lithoclasts, while muscovite, feldspar, epidote, zircon, monazite, and opaque minerals are also present. The quarzitic sandstones show regenerative incrustations around the primary rounded quartz grains. The grain boundaries are most often irregular and frequently saw-shaped, which indicates a notable meta-genetic alternation. Late veins of the fine-grained quartz aggregate are also rather frequent.

3) The third group of samples was the least numerous yet the most informative. In this case, the first sample is a cobble of pinkish quartz trachyte–alkaline intermediate volcanic rock. Large pelletized phenocrysts of potassic feldspar (up to 1 cm) and rare fine quartz grains are distributed in the groundmass composed of pelletized potassic feldspar and quartz (Fig. 8(a)). Furthermore, quartz-feldspathic myrmekites are rather frequent. There are small quantities of plagioclase, dark-colored minerals that are substituted by aggregates of chlorite, epidote, and opaque mineral.

The second sample is dolerite with typical poikilitic texture (Fig. 8(b)) formed by large poikilite clinopyroxene crystals (3-4 mm in diameter) with tabular plagioclase (up to 1-1.5 mm). There are large, separate hypidomorphic crystals of basaltic hornblende (up to 2 mm), which are substituted by hydrous ferric oxides, titanite, and chlorite. The main groundmass contains plagioclase and significant amounts of chlorite, which is presumably a product of substitution of the volcanic glass or clinopyroxene microliths.

The third sample is zoisite-amphibolite (zoisite-actinolite) metasomatic rock. Light-green idiomorphic grains of amphibole prevail over hypidomorphic crystals and sheaf-like aggregates of zoisite. Anhedral segregations of titanite and opaque ore minerals are also present. From a general chemical perspective, it can be suggested that the most probable protolith for this rock was a dolerite-like rock.

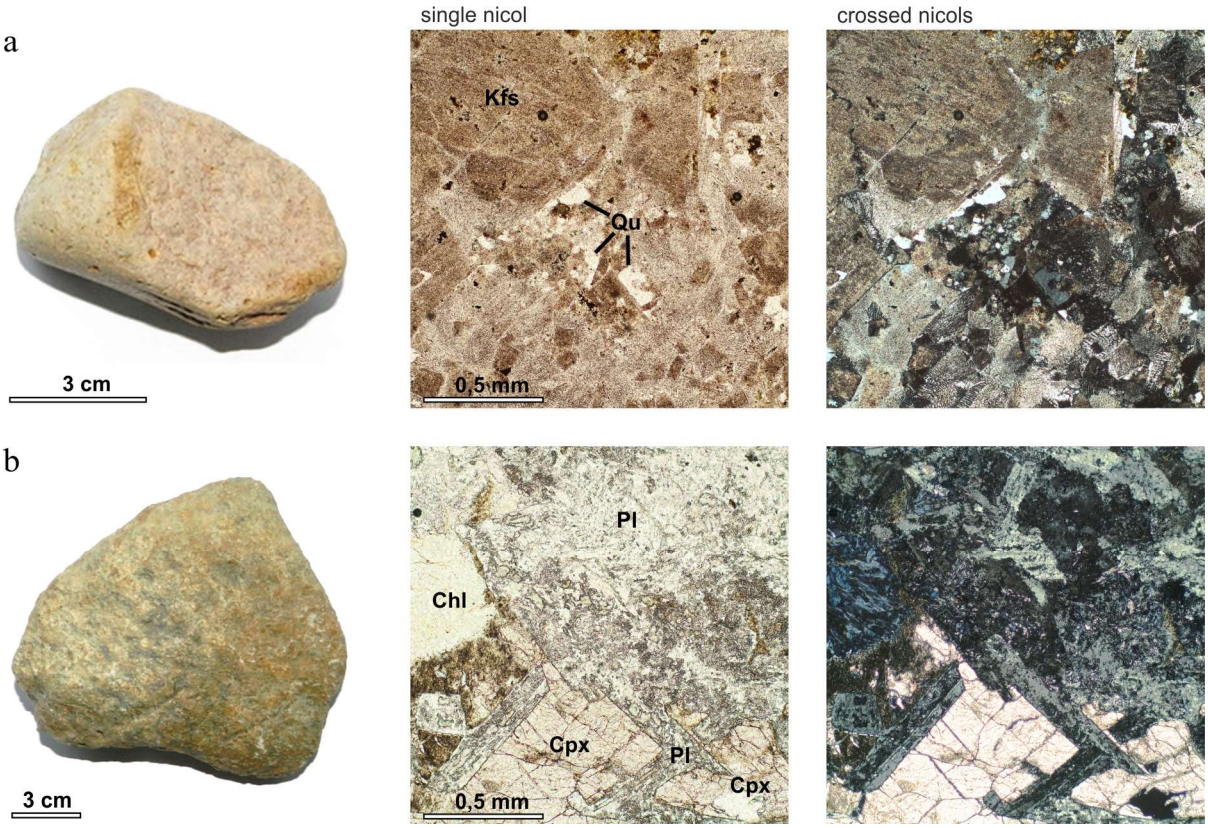

Fig. 8. (a) Sample N-10 – pinkish quartz trachyte, large inclusions of potassic feldspar (Kfs) with fine quartz grains (Qu) in the quartz-feldspathic matrix; (b) sample N-14: greenish-brown dolerite, large poikilitic clinopyroxene crystals (Cpx) with thin plagioclase crystals (Pl), in the groundmass: plagioclase chlorite (Chl)

3.5. Geomorphological Analysis

The investigated area is in the zone of sparse northern taiga with extensive peatlands. Therefore, the existing digital surface model (DSM), based on X-band radar data with high penetration capacity, reflects in detail the terrain structure of the territory. DEM mapping of the glacial ice and fluvioglacial relief features was performed using a site with an area of 54,117 km^2 as an example. Its boundaries run along the watershed of the Nadym River and its tributaries. The summary mapping results are shown in Fig. 9 and Table 4.

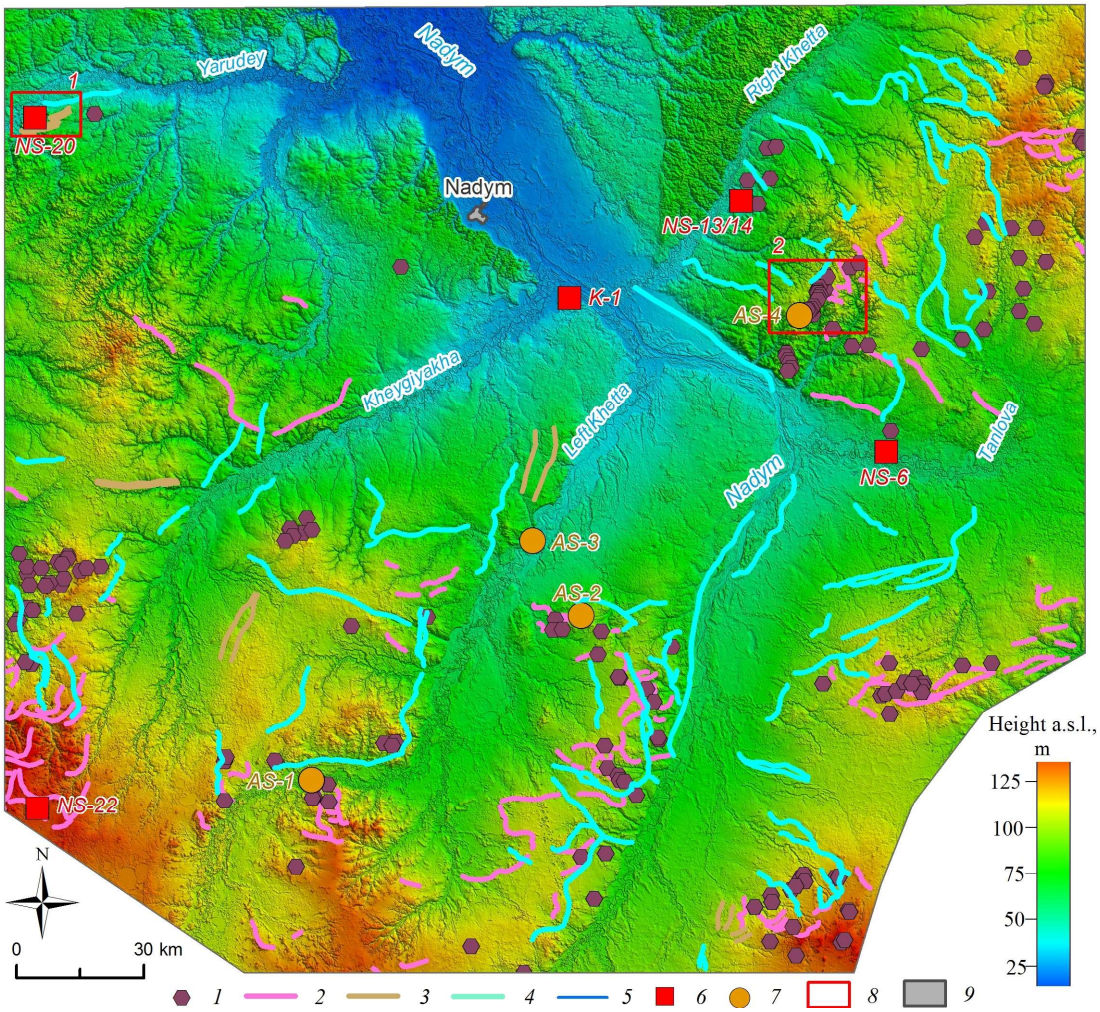

Fig. 9. Results of the glacial and fluvioglacial relief interpretation in the middle course of the Nadym River (the background image is a synthesized digital terrain model based on DEM TanDEM-X, 26 m resolution): *1: kame-like hummocks; 2: moraines; 3: parallel ridges; 4: valley trains; 5: waterways; 6: studied and sampled locations; 7: additional locations based on Khlebnikov, 1954; Yevseyev, 1958; 8: areas of typically glacial landforms; 9: settlements*

Table 4

Remote mapping of the glacial and fluvioglacial relief features in the Nadym River basin (mid and lower courses)

Relief features	Number of identified objects	Total area/length, km
Kame-like hummocks	157	-
End moraines	122	851.3
Parallel ridges	16	157.2
Valley trains	103	1411.3

Based on the map obtained (Fig. 9), it can be noted that the spread of the assumed glacial and fluvioglacial relief features within the investigated area has two distinct patterns:

– all identified features are to the south off the Yarudey and Right Khetta rivers, with individual objects found in the watershed between Yarudey and Heigiyahi (Longjugan.) In the southern and western parts, the diversity and density of the features are the highest (Tanlova and Right Khetta rivers watershed, left bank

of the Nadym River in its middle course)

– all identified features are found at the heights from 40 m a.s.l.. and higher; the density of objects significantly increases in the watershed areas above 70-75 m.

The feature of the high elevation relief distribution is demonstrated by the statistical data about the selected kameform hills. Among the 157 point objects, 145 (92%) are above 75 m, with 53 (34%) located within the narrow range of 95-104 m. Below 75 m, large objects occur individually and are poorly distinguished morphologically.

The network of extended (more than 850 km) proximal (kame) moraines that mark the final glacial massif positions is confidently recognized. They have different stretches (sub-latitudinal, north-western, etc.), which may indicate there was no single direction of the cover ice movement. In most cases, the moraines are confined to the watersheds, while they are often accompanied by other glacial forms (kames, valley trains, etc). The chain of kame hills on the watershed of the Tanlova and Right Khetta Rivers are erosive remnants of the local moraine formations, i.e. morphologically they occupy an intermediate position between the individual moraines. On the watersheds, well-drained, dry areas of sands near kame ridges are often subjected to deflation and active redispersal.

Some of the individual objects are linear ridges (about 157 km total length) The linear ridge relief also has visible signs of erosion (scours, rills, subsidences) and in most cases can be traced as a specific linear landscape texture.

The valleys and rills of the melt glacial waters flow are more than 1,400 km long. The valleys are well expressed in the southern and eastern parts of the study area and are barely visible below 40 m asl. The network of valleys does not really match the modern watercourses; they can be located both in parallel at a small distance from the ancient valleys, or intersect them at right angles. The valleys and hollows of the ancient runoff are often associated with terminal formations. The preservation of valleys is one of the key signs of marine transgression absent in the middle course of the Nadym River since the last glaciation of the region.

For clarity, two sections of typically glacial landforms are highlighted on the map (Fig. 9):

1. A site with a predominant linear ridge relief, located on the right bank of the Yarudey River (left tributary of the Nadym River), near the Nadym-Salekhard highway under construction (Fig. 10). Four long, curved ridges reaching a height of 55 m are well-preserved (the difference in relative heights is 10-12 m) To the south of the ridges stands a section of hilly, presumably kame, relief. The ridges are complicated by thermokarst and erosion features.

2. The kame hill concentration site on the right bank of the Nadym River, (Fig. 11). The kames reach an absolute height of more than 100 m (difference in relative height up to 30 m) The kames are well preserved despite the destruction of individual features by the river erosion.

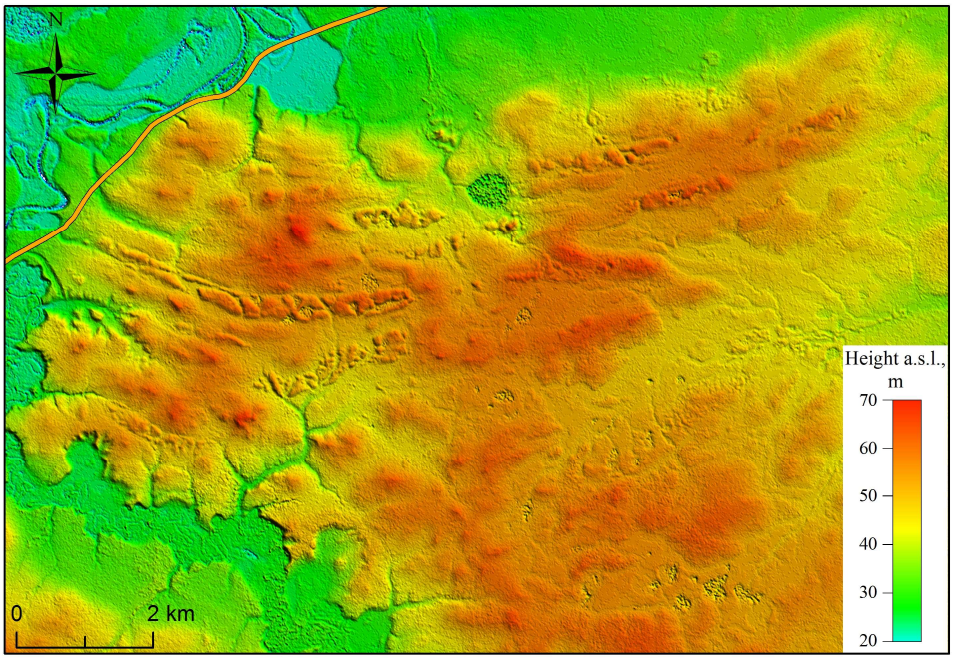

Fig. 10. Parallel ridges, DEM TanDEM-X, 12 m / pixel

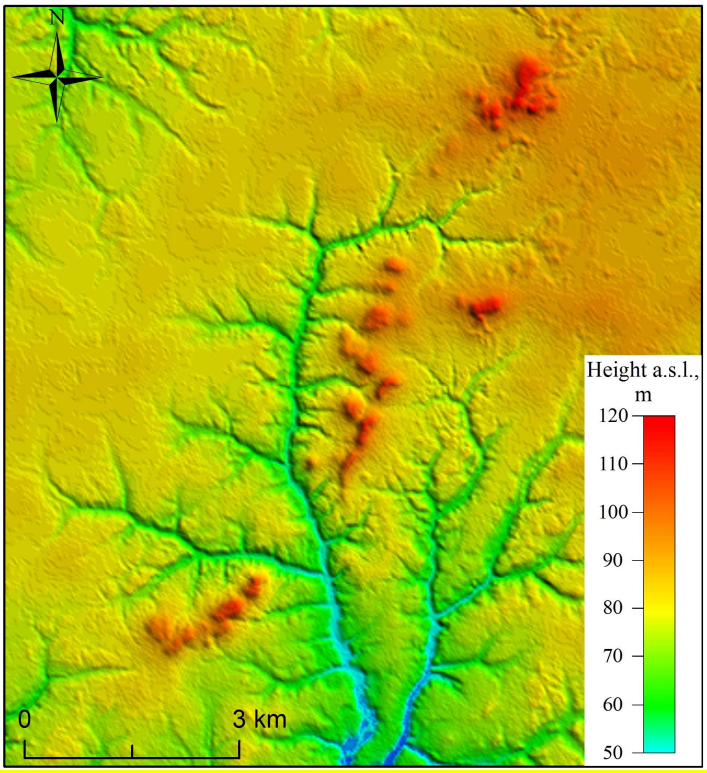

Fig. 11. Kame-like features, DEM TanDEM-X, 26 m / pixel.

5. Discussion

According to current viewpoints, the territory of the north of Western Siberia was exposed to several cover glaciations: Zyryanka (MIS 4), Taz (MIS 6) and Samarovo (MIS 8). Areas at the lower level (up to 40-45 m a.s.l.) could represent serial repeated marine transgressions in Kazantsev (MIS 5) and Karga (MIS 3) ages. in Fig. 13. Directly within the boundaries of the investigated areas the boundaries of

Taz (MIS 6) and possibly Zyryanka glaciation periods are identified (Zemtsov, 1976; Babushkin, 1996).

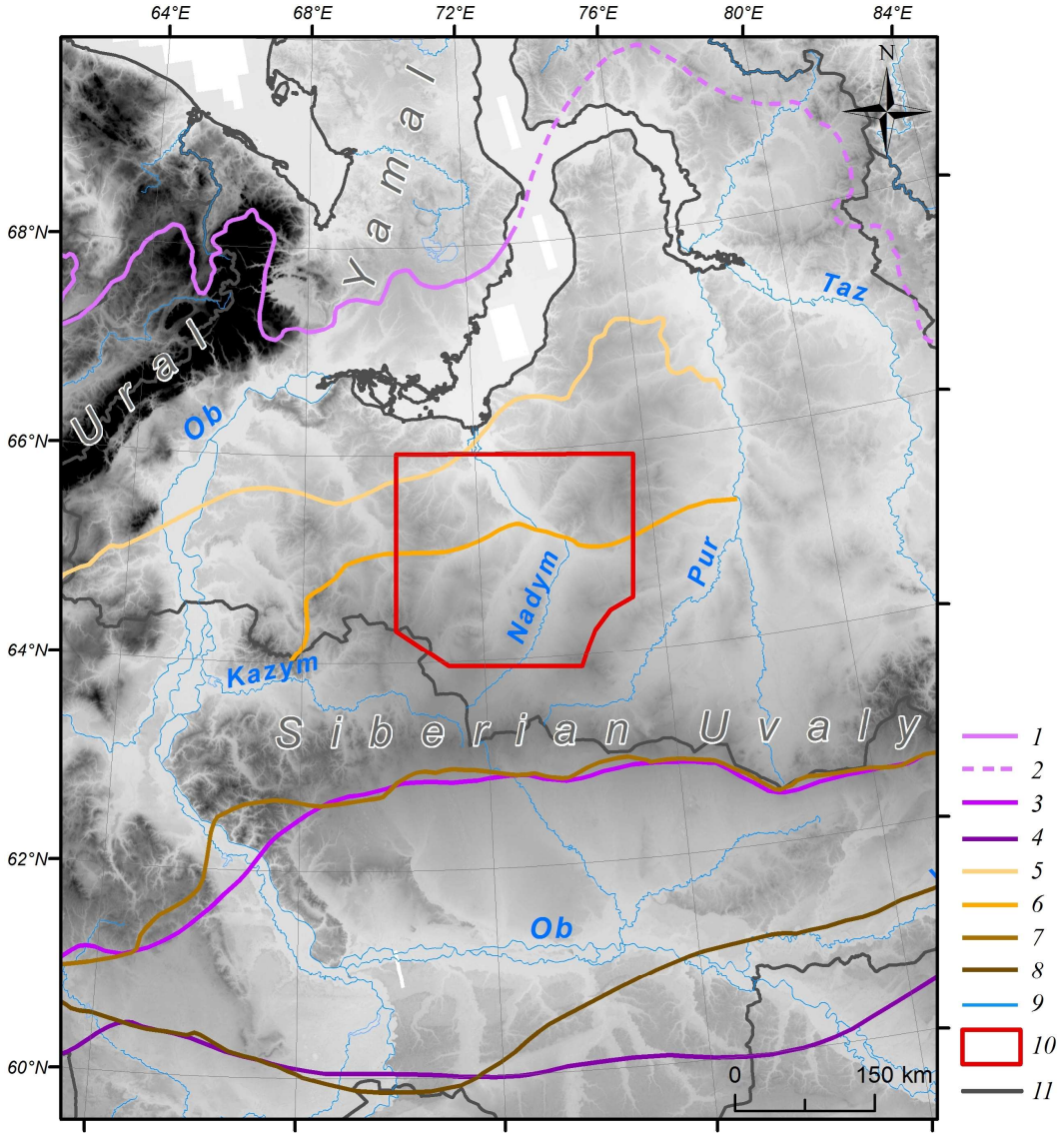

Fig. 12. 1-8: ice sheet boundaries (1: Zyryanka (Astakhov et al., 2016); 2: Zyryanka (assumed) (Astakhov et al., 2016); 3: Taz (Astakhov et al., 2016); 4: Samarovo (maximum) (Astakhov et al., 2016); 5: Zyryanka (Zemtsov, 1976; Babushkin, 1996); 6: Taz (second stage) (Zemtsov, 1976; Babushkin, 1996); 7: Taz (Zemtsov, 1976); 8: Samarovo (Zemtsov, 1976); 9: water bodies; 10: study area; 11: administrative boundaries Background: TanDEM-X 90m DEM ©DLR

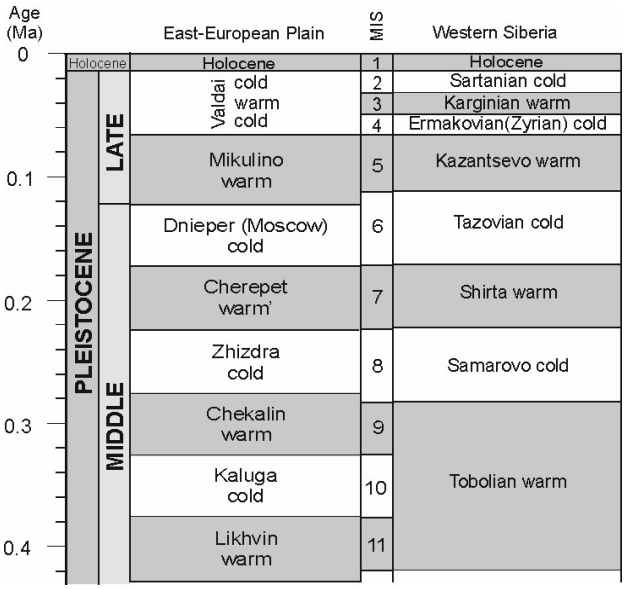

Fig. 13. Palaeoenvironmental event successions on the East-European Plain (from Bolikhovskaya, 2004; Molodkov and Bolikhovskaya, 2010) and in Western Siberia (Interregional Stratigraphic Chart..., 2014)

The key natural feature of the glacial genesis of Quaternary strata in northern Western Siberia is the presence of wrecked rock: semi-rounded angular stones, gravel and large boulders with evident glacial striation, carried over by the glacier from the territories outside the West Siberian Plain (Strelkov et al., 1965; Zemtsov, 1976). The water-glacial sediments in the research area include well-washed grey sand characterized by poor chemical composition (the gravimetric concentration of SiO_2 is 94-97%) and also containing amendments of gravel and stones (Chekunova, 1954; Groysman, 1954; Khlebnikov, 1954.). The glacial sediments include unsorted coarse-grained sands with an abundance of pebbles, as well as moraine-like bodies of lumped clay, loam, and clay sand with gravel and large boulders. The petrographic composition of boulders and pebbles includes quartz, opal, sandstones, quartz porphyres, amphibolites, granitoids, gneises and trachites. (Chekunova, 1954; Groysman, 1954; Khlebnikov, 1954.). However, it was noted that interpreting the exact location of the origin of these rocks from the geological markers representing different territories is so far problematic.

The results of the study of the sections, in general, showed that the youngest of the discussed sediments are those of the second floodplain terrace (section NS-6, K-1) In the top part, it includes aeolian sand formed no later than the beginning of the Holocene (MIS 1), in the middle part there are floodplain series of alluvium, in the lower part there are river streams of grey oblique sand of the late MIS 3 - middle MIS 2.

The absolute age of the second floodplain terrace formation of the Nadym and Tanlova Rivers (sections K-1 and NS-6) correlates well with radiocarbon and OSL datings of postglacial Pleistocene sediments throughout all the northern Western Siberia (the age ranging from 42,000 to 25,000 years) (Astakhov, Nazarov, 2010)). On average, the age of the cover formation is between 20,000 and 12,000 years (Astakhov, 2006; Zemtsov, 1976) Two types of glacial relief areas and extensive

sandur surfaces were identified on the surface of the second floodplain terrace in the large-scale field studies on the left bank of the Left Kheta River (Vasilyev, 2007).

At the middle and upper geomorphological level, grey monomineral sand with a similar age at the beginning of the NS-20 stage was also found in the NS-22 and MIS 5 sections. It can be suggested that during the Kazantsev interglacial period in the vast area of the Nadym River basin there were favorable conditions for the erosion of the previously accumulated sandy textured deposits and their transfer downstream the main rivers.

One of the most interesting points of research is the kameform hill on the left bank of the Right Khetta River (NS-13/14), the formation of its middle part corresponds to the Tobol interglacial period (MIS 9-11). It can be suggested that the sediments in the upper part of the hill are not younger than the Taz glaciation (MIS 6), while the pebble layer formed during the degradation of the glacier reinforced the previous sediments and later was resistant to erosion, and was not covered by the waters of the Kazantsev and Karga transgressions

The results of the sand quartz grain morphology analysis confirmed the supposed genesis of the studied sections. Thus, for sections NS-6 and K it was shown that in the upper part of sections the sequence is: aeolian sediments, aluvial flood plain facies, and channel facies of coarse stratified sands. At the base of both sections, there are sediments in which, apart from typically river grains, a large number of various morphology grains are found. These are grains of varying degree of roundness, irregular shape with a smooth surface and smooth faces, often on their surface, there are various grooves and scratches formed under the strong mechanical impact, as well as conchoidal fractures. Their origin could be a result of freezing weathering and cryogenic transformation (Velichko and Timireva, 1995), as well as of high pressure applied to the grain surface (Immonen et al., 2014; Vos et al., 2014;) Well-rounded ellipsoid and ball-shaped grains predominate in the top layer sediments. One can associate this distribution with materials coming from two different sources. One source could have been the former glacial sediments eroded by fluvial processes. This type of terrace structure corresponds well with the results of the study by Velichko et al. (2011) who analyzed sands with underlay peat deposits in the investigated region.

Quartz grains from sections NS-13/14 and NS-20 are often characterized by low rounding classes, multiple conchoidal fractures, sometimes even conchoidal systems, a deep-pitted surface, scratches, grooves, and cleavage surfaces. Such elements could be signs of processes that occur in glacial environments. Often, there are also signs of subsequent water treatment: separate crescentic depressions and smoothed sharp peaks of grains. It indicates the redeposition of the glacial grains by water flows. Along with the grains described above, there are also typical subaquatic grains: well-rounded with a fine-pitted surface, but their number is inferior to grains with glacial features.

Currently, we lack sufficient evidence to confirm the glacial genesis of these deposits. It is possible that the grains were exposed to the effects of glacial processes, with a final processing phase in their history that included subaquatic processes. In section NS-22, the grain morphology provides evidence that suggests the existence

of a quiet subaquatic environment under which quartz grains underwent long-term treatment.

In general, the results of sand quartz grain morphoscopy and morphometry show that most quartz grains from all sections underwent complex multi-stage processing throughout their life.

The petrographic diversity of erratic boulders in West Siberia helps us distinguish two or three paleoglacial regions that combine several dozen distributed provinces. Each is characterized by a specific set of rocks and petrographic features. The first major generalization in this respect was made by Zemtsov (1976), who identified the guide boulders of the Ural region as ultramafic and mafic rocks of the Main (axial) Uralian zone, plagio-granites, and highly metamorphosed rocks (gneisses and shales). In the Central Siberian region, the prevailing boulders include dolerites and basalts of the Putorana Plateau, as well as various granitoids, quartzites, and Palaeozoic sandstones of the Taimyr Region. These studies were substantially supplemented and detailed work by Sukhorukova et al. (1987).

Despite their small quantity, the petrographic analysis of pebbles and boulders led to the following conclusions. First, high-silica alkaline effusive rocks (sample N-10, quartz trachyte) are indicative of both the Northern Taimyr Province (Troitsky and Shumilova, 1973) and many moraines of the Ural paleoglacial region (Sukhorukova et al., 1987), but they are never found in the Putorana Plateau and the southmost regions. Moreover, there is only a small relative share of dolerites (sample N-14, dolerite) and other effusive mafic rocks, which is a property of Putorana and Nizhnyaya Tunguska regions. In contrast, there is no limestone that would be typical of the Central Siberian paleoglacial region (Kulyumbinsk and Sukhaya Tunguska distributive provinces according to Sukhorukova et al., 1987). There is no granite in the samples either, which is a property of the Northern Taimyr region.

Second, quartz and quartzite sandstones are typical for the Ural paleoglacial region, but their share is usually within a few per cent. Quartzitic sandstones also described as Palaeozoic were found 50 km north of Surgut within the tentative Central Siberian and Middle rock outwash zones (Sukhorukova et al., 1987). The source of the polymictic platy jointing sandstone could be the Palaeozoic bordering of the eastern slope of the Urals (Sukhorukova et al., 1987) or the Mesozoic sandstone of the West Siberian Plate.

In general, the samples have a significant proportion of terrigenous rocks (sandstones and siltstones) and low content of dolerites. On the one hand, this can be explained by the poor representativeness of the samples. Nevertheless, the key washout zone could be located further north than the Putorana Plateau in the Taimyr area. To substantiate this point of view, further research is planned to determine the trace element composition and absolute dating and to expand the sampling.

Despite the numerous features that make it possible to attribute the thickness of grey monomineral quartz sand (K-1, NS-6, NS-20) to fluvioglacial sediments, and the upper pebble strata of section NS-13/14 to glacial sediments, the study did not find typical moraine-like formations of lumped clay, loam and clay sand with gravel and large boulders in this territory. However, detailed descriptions of this type of

685 sediment can be found in some references (Strelkov S.A. et al., 1965; Zemtsov,
686 1976; Sukhorukova et al., 1987; Babushkin, 1996 и др.).
687 Thus, in the middle course of the Right Khetta River at Point 70 (Khlebnikov,
688 1954)2.5 m deep there is a 20 m-thick until of densely clumped loam with interlayers
689 of mica enriched sand (the layers are up to 25 cm thick) (section AS-1, Fig. 9). The
690 color of the loam is brown, small glitter mica is visible, and angular debris (granite)
691 are found, up to 25 cm in diameter. In the right part of the section upstream, stripping
692 exposed a layer of fine-grained sand. Below 15 m it is followed by an interlayer of
693 gravel-pebble rock. The prominent colluvium slope is covered by loam crushed
694 stone, and a cluster of gravel-pebble rock is also found on the towpath.
695 It has a wide extension and rises up to 25-30 m above the surrounding plain.
696 The ridge part of the range is convex and consists of individual peaks separated by
697 meso ridges. On the surface of the ridge, the congestion of pebble and gravel is
698 found. The gravel-pebble coarse-grained well-washed and leached sand is traced
699 down to the depth of 1.2 m.
700 Two esker-like linear elevations and a small kameform hill were discovered
701 in the lower course of the Right Khetta River at well No. 18 (Khlebnikov, 1954) at
702 1.8 m depth in the gravel-pebble horizon with a total depth of 17.6 m (section AS-3,
703 Fig. 9) The diameters of the pebbles are between 0.5 and 3-4 cm. The pebbles are
704 not rounded and consist mainly of quartz and sandstone.
705 The moraine hills in the upper part of the Bolshoy Huhu River (right tributary
706 of the Nadym River) have a north-west and a north-east orientation. The length
707 reaches 6-7 km, and the relative height varies from 15 to 60 m. (Chekunova, 1954;
708 Yevseyev, 1958)morphologically, the steep slopes of the hills have individual
709 smoothed tops separated by small saddles. The upper layer of the hills to a depth of
710 1-2 m is peeled loam with abundant pebble rock. The pebbles are weak and poorly
711 rounded, and their diameters do not exceed 2-4 cm. Petrographic composition in one
712 of the sections reveals (so-called point 367 (Chekunova, 1954)): silica, clay shale,
713 arkoses sandstones, breccia of clay-quartz rocks and limonite. The results of manual
714 drilling at some small hills (Yevseyev, 1958; Andreev, 1960) showed that they are
715 folded with permafrost sediments. The total ice content as determined visually is not
716 less than 30%. As an example, well No. 10 (Yevseyev, 1958), where light grey clay
717 with yellowish color, light, porous, with alevrite interlayers is found at a depth of
718 1.4-10.7 m, has a wavy and horizontal lamination (section AS-4, Fig. 9.) Clay
719 thickness is underlayed with grey clay fine-grained sands with poor sorting and
720 admixture of gravel grains, quartz, and silicon pebbles.
721 Data from both our studies and previous field studies are in good
722 correspondence to the results of the analyses with the Tandem-X Digital Terrain
723 Models. These models revealed that despite the plain origin of the territory, the high
724 salinity and dominance of erosion processes, various glacial and fluvioglacial relief
725 features preserved to various degrees (kameform hills, proximal moraines, and linear
726 elevations, glacial meltwaters etc.) are evident.
727 A linear-oriented relief caused by a glacial impact in northern Western Siberia
728 is highlighted on the Map of Quaternary Formations in Russia, 1:2,500,000 scale
729 (Astakhov et al. 2016). At the same time, linear features and glacial remains are

identified on geological maps of larger scales (Babushkin, 1995).

Nowadays, due to the increasing availability of initial DTM data, remote mapping of glacial relief features become the standard method across the world (Clark et al. 2004; Glasser et al. 2008; Sharpe et al. 2010; Atkinson et al. 2014; Norris et al. 2017). Based on modern spatial data, a detailed map for the British Isles Territory and Coastal Zone (BRITICE-2) is available for digital study and analysis, and was updated (Clark et al., 2018). The remote features of most forms of glacial relief for various natural conditions are described in detail and offer numerous evidence that can be used as standards for remote sensing data interpretation, including the entire north area of Western Siberia.

6. Conclusions

Our results showed high efficiency of simultaneous application of field ground and remote methods even with limited raw site rocks. Sediments were identified, which can be immediately attributed to fluvioglacial (lower part of section K-1 and NS-6, section NS-20) and glacial (upper layer of section NS-13/14) origins. Traces of glacial treatment were also found as landforms in certain areas such as kameform hills, proximal moraines, linear-bed elevations, depressions of melt glacial water runoffs. Due to low organic substance content, sparse lichen- pine trees are formed over the fluvioglacial sediments on the low-fertile podzolic soils. It is a characteristic landscape feature of the leaching soil condition for the north taiga in Western Siberia. At the same time, the moraine-like layers of aggregated clay, loam and clay sand with gravel and large stone boulders that could not be found in field studies are widely described in sources previously unpublished (particularly the Left Khetta and in the upper reaches of the Great Huhu River)

Thus, the development history of the Nadym River lower stream area provides evidence that periods of cover glaciations occurred here in the Pleistocene. At the same time, it is difficult to say whether it was a single glacier with a common front, or whether there were several separate centers of ice accumulation. The available data, especially the structure and functional characteristics of the relief, appear to favor the second option, at least in the late Pleistocene. In the early periods, traces of larger glaciation may represent the vast lake-alluvial plains and flood plains, reaching a maximum area in the basin of the Nadym, Pur and Taz rivers. In this case, they can be considered as the latest erosion formations but preserved a characteristic structure inherited by modern landscapes.

7. Acknowledgements

The authors thank the Terrasar-X (DLR) research team for providing the TanDEM DTM for research (DEM_GEOL1378). We also thank the anonymous reviewers whose comments and suggestions helped improve and clarify this manuscript.

This study was funded by the RFBR and the Yamal-Nenets Autonomous District, project number 19-45-890008. The investigation is under a public assignment by the Institute of Geology and Mineralogy, Siberian Branch, Russian Academy of Sciences.

References

Alyavdin F.A., and Mokin N.P.: Geological map. 1rd ed. Scale 1:1,000,000. Ministry of Geology and Subsoil Protection of the USSR, Map Q-43 (Novyy Port.) Gosgeoltekhizdat, Moscow, 1957.

Andreev Yu.F. About the relationship of linear-ridge topography with tectonic structures in the north of Western Siberia (in the field of permafrost development.) Geologiya i geokhimiya. Geology and geochemistry, 3(IX), 76–94, 1960.

Astakhov, V.I.: On chronostratigraphic units of the Upper Pleistocene in Siberia, Geologiya i geofizika, 47(11), 1207–1220, 2006.

Astakhov, V., Nazarov, D. Correlation of Upper Pleistocene sediments in northern West Siberia. Quaternary Science Reviews, 29(25-26), 3615–3629., 2010.

Astakhov, V., Shkatova, V., Zastrozhnov, A. and Chuyko, M.: Glacio-morphological Map of the Russian Federation, Quaternary International, 420, 4–14, 2016.

Atkinson, N., Utting, D., and Pawley, S.: Landform signature of the Laurentide and Cordilleran ice sheets across Alberta during the last glaciation. Canadian Journal of Earth Sciences, 51(12), 1067-1083, doi: 10.1139/cjes-2014-0112, 2014

Babushkin, A.E.: Quaternary map. 2rd ed. Scale 1:1,000,000. Russian Federation Committee on Geology and Mining (Roskomnedra), Map Q-42,43 (Salekhard.) St. Petersburg: VSEGEI Cartographic Factory, 1996.

Bolshiyanov, D.Yu.: Passive Glaciation of the Arctic and Antarctic Regions. AANII, Saint Petersburg, 296 p, 2006.

Chekunova, V.S.: Geological and geomorphological survey of a part of the lower reaches of the Nadym River basin and parts of the right bank of the Nadym Ob River. VSEGEI, Leningrad, 1954.

Clark, C, Evans, D, Khatwa, A., Bradwell, T., Jordan, C., Marsh, S., Mitchell, W., and Bateman, M.: Map and GIS database of glacial landforms and features related to the last British ice sheet. Boreas, 33, 359–375, 2004.

Clark, C, Ely, J, Greenwood, S, Hughes, A, Meehan, R, Barr, I, Bateman, M, Bradwell, T, Doole, J, Evans, D, Jordan, C, Monteys, X, Pellicer, X, Sheehy, M.: BRITICE Glacial Map, version 2: a map and GIS database of glacial landforms of the last British–Irish Ice Sheet. Boreas, 47, 11–27, 2018.

Bolikhovskaya, N. S.: Paleoenvironments and climato-stratigraphy of the loess-paleosol formation of Northern Eurasia. 4, 11–36, 2004.

Faibusovich, Ya. E. and Abakumova L.A. Map of Pliocene-Quaternary formations. 3rd ed. Scale 1:1,000,000. Federal Agency for Subsoil Use (Rosnedra), Map Q-43 (New Urengoy.) St. Petersburg: VSEGEI Cartographic Factory, 2015.

Fredin, O., Rubensdotter L., Welden, A., Larsen, E. and Lysa, A.: Distribution of ice marginal moraines in NW Russian, Journal of Maps, 8(3), 236–241, 2012. doi: 10.1080/17445647.2012.708536

Glasser, N., Jansson, K., Harrison, S., and Kleman, J.: The glacial geology and Pleistocene history of South America between 38,8S and 56,8S. Quaternary Science Reviews, 27, 365–390, 2008.

Grosvald, M.G.: Eurasian Hydrospheric Catastrophes and Glaciations of the Arctic Region, Nauchny Mir, Moscow, 1999.

Groysman, Ya.M.: Geological survey of the Haigi-Yakh River basin (Long-Yugan). VSEGEI, Leningrad, 1954.

Generalov, P.P.: Upper Pleistocene of the lower course of the Ob River In: Collection of scientific papers of the West Siberian Scientific and Research Geological Prospecting Petroleum Institute, Tyumen, 56–77, 1986.

Immonen, N., Strand, K., Huusko, A., and Lunkka, J.P.: Imprint of late Pleistocene continental processes visible in ice-rafted grains from the central Arctic ocean. Quaternary Science

827 Reviews 92, 133–139, 2014.
828 Interregional stratigraphic chart of the Quaternary of the territory of the Russian Federation.
829 Interdepartmental Stratigraphic Committee, VSEGEI, St. Petersburg, 2014.
830 Kalinska-Nartisa E., Woronko B., and Ning Wenxin. Microtextural inheritance on quartz sand
831 grains from Pleitocene periglacial environments of the Mazovian Lowland, Central Poland.
832 Permafrost and Periglacial Processes 28, 741–756, 2017.
833 Khabakov, A.V.: On roundness indexes of pebble, Sovetskaya Geologiya, 10, 98–99, 1946.
834 Khlebnikov, V.I.: Geological and geomorphological survey of a part of the middle reaches of the
835 Nadym river basin. VSEGEI, Leningrad, 1954.
836 Krinsley, D.H., and Doornkamp, J.C.: Atlas of quartz sand surface textures. 2nd edition.
837 Cambridge, Cambridge University Press, 102, 2011.
838 Kind, N.V.: Late Quaternary Geochronology According to Isotope Data. Nauka, Moscow, 1974.
839 Lazukov, G.I.: Antopogen of the northern part of Western Siberia (Paleogeorgaphy), Moscow, 127
840 p, 1972.
841 Maslennikov, V.V.: Regional Geo-Ecological Mapping at Scale of 1:1000000 Within the North
842 End of Tyumen Oblast. Labytnangi, 1998.
843 Molodkov, A.: The Late Pleistocene palaeoenvironmental evolution in Northern Eurasia through
844 the prism of the mollusc shell-based ESR dating evidence. Quaternary International, (in
845 press.), 2020.
846 Molodkov, A.: Cross-check of ihe dating results obtained by ESR and IR-OSL methods:
847 implication for the Pleistocene palaeoenvironmental reconstructions. Quat. Geochronol., 10,
848 188–194, 2012.
849 Molodkov, A., and Bolikhovskaya, N.: Climato-chronostratigraphic framework of Pleistocene
850 terrestrial and marine deposits of Northern Eurasia based on pollen, electron spin resonance,
851 and infrared optically stimulated luminescence analyses. Est. J.Earth Sci. 59(1), 49–62,
852 2010.
853 Molodkov, A., and Bitinas, A.: Sedimentary record and luminescence chronology of the
854 Lateglacial and Holocene aeolian sediments in Lithuania. Boreas, 35 (2), 244–254, 2006.
855 Copernicus Open Access Hub (n.d.) Available at: https://scihub.copernicus.eu/dhus/#/home
856 Norris, S. L., Margold, M,. and Froese, D.G.: Glacial landforms of northwest Saskatchewan.
857 Journal of Maps, 13, 600–607, doi:10.1080/17445647.2017.1342212, 2017.
858 Rukhin, L.B.: Fundamentals of Lithology. Doctrine of Sedimentary Rocks. Nedra, Leningrad,
859 1969.
860 Rusakov, A., Sedov, S., Sheinkman, V., Dobrynin, D., Zinovyev, E., Trofimova, S. and
861 Levchenko, S.: Late Pleistocene paleosols in the extra-glacial regions of Northwestern
862 Eurasia: Pedogenesis, post-pedogenic transformation, paleoenvironmental inferences.
863 Quaternary International. 501, 174-192, doi:10.1016/j.quaint.2018.03.020, 2018.
864 Sharpe, J., Sharpe, D., and Harris J.: A flowline map of glaciated Canada based on remote sensing
865 data. Canadian Journal of Earth Sciences, 47, 89–101, 2010.
866 Sedov, S., Rusakov, A., Sheinkman, V., and Korkka, M.: MIS3 paleosols in the center-north of
867 Eastern Europe and Western Siberia: Reductomorphic pedogenesis conditioned by
868 permafrost? Catena, 146, 38–47, doi:10.1016/j.catena.2016.03.022, 2016
869 Sheinkman, V., Sedov, S., Shumilovskikh, L., Korkina, E., Korkin, S., Zinovyev, E. and Golyeva,
870 A.: First results from the Late Pleistocene paleosols in northern Western Siberia:
871 Implications for pedogenesis and landscape evolution at the end of MIS3. Quaternary
872 International, 418, 132–146, doi:10.1016/j.quaint.2015.12.095, 2016.
873 Sizikova, A.O. and Zykina V.S.: The dynamics of the Late Pleistocene loess formation, Lozhok
874 section, Ob loess Plateau, SW Siberia. Quaternary International, 365, 4–14, 2015.
875 Strelkov S.A., Saks V.N., Arkhipov S.A., Volkova V.S. The problem of the Quaternary glaciations
876 of Siberia. The main problems of the study of the Quaternary period, Nauka, Moscow, 188–
877 205, 1965.
878 Svendsen, J., Alexahderson, H., Astakhov, V., Demidov, I., Dowdeswell, Ju., Funder, S., Gataulin,

879 V., Henriksen, M., Hjort,H., Houmark-Nielsen, M., Hubberten, H.-W., Ingolfsson,
880 O.,Jakobsson, M., Kjar, K., Larsen, E., Lokrantz, H., Lunkka, Ju. P.,Lysa, A., Mangerud, J.,
881 Matiouchkov, A., Murray, A., Moller, P., Niessen, F., Nikolskaya, O., Polyak, L., Saarnisto,
882 M., Siegert, Ch., Siegert, M., Spielhagen, R., and Stein, R.: Late Quaternary ice sheet history
883 of Northern Eurasia. Quaternary Science Reviews, 23 (11-13), 1229–1271, 2004.
884 Sukhorukova, S.S., Kostyuk M.A., Podsosova, L.L., Babushkon A.E., Zolnikov, I.D., Abramova,
885 S.A. and Goncharov, S.V.: Moraines and Dynamics of Glaciation in Western Siberia. Works
886 of Institute of Geology and Geochemistry of the Siberian Branch of the USSR Academy of
887 Sciences, Issue 672. Nauka, Novosibirsk, 1987.
888 Troitskiy, S.L. and Shumilova, E.V.: Stratigraphy and Mineralogical-Petrographic Peculiarities of
889 Quaternary Deposits in the Vorontsov Yar Stratum in the Lower Course of the Yenisei River.
890 In: Lithology and Conditions of Formation of the Quaternary Deposits of the Northern
891 Eurasia, Institute of Geology and Geochemistry of the Siberian Branch of the USSR
892 Academy of Sciences, Novosibirsk, 5–37, 1974.
893 Vasilyev, S.V.: Forest and Bog Landscapes of Western Siberia. Izdatelstvo NTL, Tomsk, 2007.
894 Velichko, A.A. and Timireva S.N.: Morphoscopy and morphometry of quartz grains from loess
895 and buried soil layers, GeoJournal, 36(2/3), 143–149, 1995.
896 Velichko, A.A., Timireva, S.N., Kremenetski, K.V., McDonald, G.M. and Smith, L.C.: West
897 Siberian Plain as a late glacial desert, Quaternary International, 237 (1-2), 45–53, 2011.
898 Velichko, A.A.: Current state of conceptions on continental glaciers of the Earth. Bulletin of the
899 Academy of Sciences of the USSR, Geographical Series, 3, 21–34, 1987.
900 Velichko, A.A., Kononov, V.M. and Faustova M.A.: The last glaciation of Earth: size and volume
901 of ice-sheets, Quaternary International, 41 (42), 43–51, 1997.
902 Vos, K., Vandenberghe, N. and Elesen, J.: Surface textural analysis of quartz grains by scanning
903 electron microscopy (SEM): From sample preparation to environmental interpretation,
904 Earth-Science Reviews, 128, 93–104, 2014.
905 Woronko, B.: Frost weathering versus glacial grinding in the micromorphology of quartz sand
906 grains: Process and geological implications. Sedimentary Geology, 335, 103–119, 2016.
907 Zemtsov, A.A.: Geomorphology of the West Siberian Plain (Northern and Central Parts),
908 Publishing house of the Tomsk State University, Tomsk, 1976.
909 Yevseyev, G.P., and Reynin, I.V.: Geological structure and geomorphology of the Tanlova,
910 Right Khetta, and Big Huhu basins (right tributaries of the middle segment of the Nadym river).
911 VNIGRI, Leningrad, 1958.
912

9. Annexes

Annex 1. Bulk content of chemical elements

Sampling depth, m	Sample No	Bulk content, %							
		SiO_2	Al_2O_3	Fe_2O_3	K_2O	Na_2O	P_2O_5	CaO	TiO_2
K-1									
0.1	S1	87.65	5.27	0.95	1.66	1.00	0.03	0.51	0.64
0.35	S2	88.09	5.14	1.89	1.14	0.56	0.05	0.32	0.53
1	S3	89.49	4.93	1.20	1.52	0.75	0.04	0.41	0.41
1.8	S4	92.97	3.35	0.61	1.32	0.51	0.02	0.27	0.21
2.3	S5	90.71	4.21	0.92	1.35	0.64	0.03	0.38	0.39
3	S6	98.02	0.88	0.30	0.25	0.07	0.01	0.10	0.10
4	S7	98.39	0.69	0.25	0.20	<0.05	0.01	0.08	0.08
NS-6									
0.3	S1	90.60	6.20	0.87	0.91	0.63	0.08	0.28	0.37
0.7	S2	91.85	4.57	0.74	1.47	0.58	0.01	0.41	0.37
1.4	S3	93.22	3.92	0.51	1.15	0.57	0.01	0.31	0.25
3.2	S4	92.37	4.05	0.75	1.38	0.62	0.02	0.43	0.35
4	S5	90.32	5.39	0.98	1.74	0.62	0.02	0.46	0.47
4.2	S6	97.33	1.54	0.26	0.15	0.45	0.00	0.18	0.08
4.6	S7	89.79	5.86	0.95	1.80	0.65	0.03	0.63	0.35
5	S8	96.65	1.88	0.28	0.42	0.49	0.01	0.20	0.11
7.4	S9	97.29	1.46	0.24	0.25	0.48	0.01	0.16	0.07
9.2	S10	97.78	1.19	0.21	0.07	0.45	0.01	0.17	0.07
NS-13/14									
1.1	S1	97.72	1.43	0.21	0.00	0.43	0.00	0.14	0.10
3.1	S2	91.00	1.26	5.62	0.00	0.63	1.28	0.16	0.07
3.5	S3	96.58	1.22	1.14	0.15	0.56	0.12	0.18	0.11
4	S4	98.14	0.99	0.15	0.00	0.48	0.00	0.15	0.07
4.3	S5	96.25	1.18	1.58	0.07	0.47	0.06	0.16	0.24
4.75	S6	92.75	1.23	5.08	0.01	0.64	0.02	0.18	0.12
5	S7	98.34	0.89	0.17	0.00	0.43	0.00	0.13	0.09
NS-20									
1.5	S1	95.61	1.79	0.39	0.48	0.08	0.02	0.08	0.44
3.7	S2	95.59	1.83	0.21	0.68	0.09	0.01	0.07	0.16
6.5	S3	97.12	1.14	0.19	0.39	0.09	0.01	0.07	0.10
9.5	S4	94.30	2.31	0.31	0.84	0.10	0.02	0.07	0.38
16.45	S5	97.26	0.93	0.22	0.22	0.05	0.01	0.07	0.20
NS-22									
1.1	S1	96.49	1.53	0.32	0.61	0.17	0.01	0.11	0.17

Annex 2

Spearman's coefficients of correlation

	SiO_2	TiO_2	Al_2O_3	Fe_2O_3	MnO	MgO	CaO	Na_2O	K_2O	P_2O_5	BaO
SiO_2	1	-1	-1	-0.89	-0.84	-0.76	-0.89	-0.89	-0.79	-0.81	-0.62
TiO_2	-1	1	1	0.89	0.94	0.75	0.89	0.89	0.79	0.83	0.73
Al_2O_3	-1	1	1	0.89	0.94	0.78	0.89	0.89	0.79	0.84	0.73
Fe_2O_3	-0.89	0.89	0.89	1	0.93	0.95	0.75	0.75	0.61	0.97	0.61
MnO	-0.84	0.94	0.94	0.93	1	0.86	0.85	0.85	0.76	0.91	0.78
MgO	-0.76	0.78	0.78	0.95	0.86	1	0.67	0.67	0.52	0.99	0.54
CaO	-0.89	0.89	0.89	0.75	0.85	0.67	1	1	0.96	0.71	0.91
Na_2O	-0.89	0.89	0.89	0.75	0.85	0.67	1	1	0.96	0.71	0.91
K_2O	-0.79	0.79	0.79	0.61	0.76	0.52	0.96	0.96	1	0.56	0.96
P_2O_5	-0.81	0.83	0.84	0.97	0.91	0.99	0.71	0.71	0.56	1	0.59
BaO	-0.62	0.73	0.73	0.61	0.78	0.54	0.91	0.91	0.96	0.59	1

Significance level $p<0.05$

923 Annex 3. Grain size distribution

Sampling depth	Sample	Fraction size (mm) / Content (%)					
		Silt and clay	Very fine sand	Fine sand	Medium grained sand	Coarse Sand	Very coarse sand
K		***<0.09***	***0.125-0.09***	***0.25-0.125***	***0.5-0.25***	***1-0.5***	***>1***
0.1	S1	31.7	29.2	28.7	9.5	0.7	0.1
0.35	S2	18.7	12.5	32.1	32.2	4.2	0.3
1	S3	18.9	32.3	35.6	11.9	1.2	0.1
1.8	S4	5.9	20.1	56.7	16.4	0.9	0.0
2.3	S5	5.6	13.1	59.9	19.8	1.6	0.0
3	S6	0.6	0.4	1.8	71.5	23.7	1.9
4	S7	0.4	0.5	4.2	46.3	46.9	1.7
NS-6		***<0.075***	***0.10-0.075***	***0.25-0.10***	***0.5-0.25***	***1-0.5***	***>1***
0.3	S1	11.0	6.6	52.7	26.9	2.8	0.0
0.7	S2	0.8	6.8	70.8	18.7	0.4	1.9
1.4	S3	2.0	8.8	65.8	21.2	1.3	0.5
3.2	S4	3.6	8.4	72.8	15.2	0.0	0.0
4	S5	29.9	14.9	50.2	5.1	0.0	0.0
4.2	S6	2.8	0.0	29.4	61.9	5.9	0.0
4.6	S7	26.2	21.1	51.1	1.6	0.0	0.0
5	S8	0.0	0.0	41.1	55.0	3.9	0.0
7.4	S9	1.1	0.1	29.2	52.1	17.4	0.0
9.2	S10	0.5	0.0	29.4	57.5	12.6	0.0
NS-13/14		***<0.075***	***0.10-0.075***	***0.25-0.10***	***0.5-0.25***	***1-0.5***	***>1***
1.1	S1	0.0	0.0	0.6	37.4	58.0	4.0
3.1	S2	8.0	0.0	0.3	36.6	54.2	0.9
3.5	S3	5.9	0.0	10.6	59.9	23.6	0.0
4	S4	0.0	0.0	7.1	62.9	30.0	0.0
4.3	S5	24.4	1.2	15.3	40.9	18.0	0.1
4.75	S6	1.9	0.0	6.5	53.5	37.5	0.6
5	S7	0.0	0.0	8.0	61.5	30.6	0.0
NS-20		***<0.09***	***0.125-0.09***	***0.25-0.125***	***0.5-0.25***	***1-0.5***	***>1***
1.5	S1	0.0	2.2	62.1	21.9	1.3	12.5
3.7	S2	0.0	4.3	72.0	23.0	0.5	0.2
6.5	S3	0.0	4.4	55.8	38.5	1.1	0.3
9.5	S4	0.0	9.3	70.7	16.0	1.5	2.4
16.45	S5	0.0	0.9	56.8	37.6	4.0	0.6
NS-22		***<0.09***	***0.125-0.09***	***0.25-0.125***	***0.5-0.25***	***1-0.5***	***>1***
1.1	S1	0.0	1.4	53.3	44.3	0.9	0.1

924
925
926

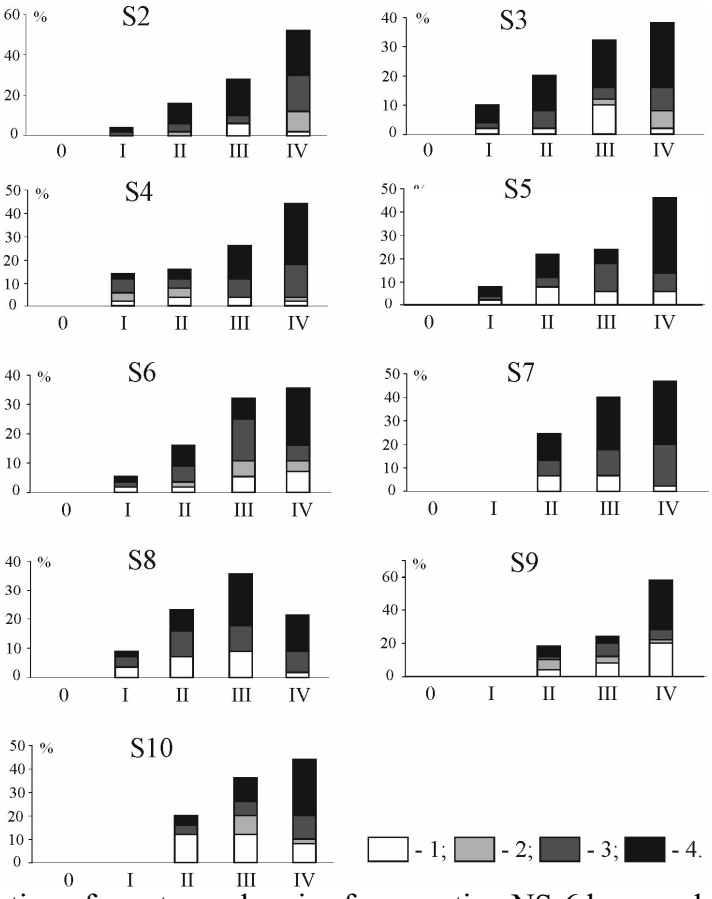

Annex 4. Distribution of quartz sand grains from section NS-6 by roundness and dullness. 1:glossy; 2:quater-matte; 3:half-matte; 4: matte; 0, I, II, III, IV are grades of roundness according to Khabakov (1946)

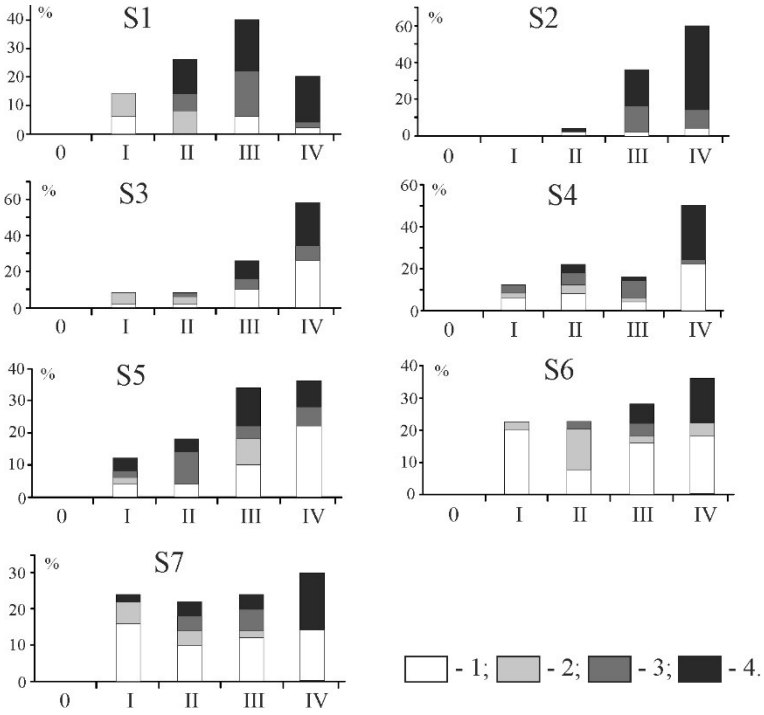

Annex 5. Distribution of quartz sand grains from section NS-6 by roundness and dullness. 1:glossy; 2:quater-matte; 3:half-matte; 4: matte; 0, I, II, III, IV are grades of roundness according to Khabakov (1946)

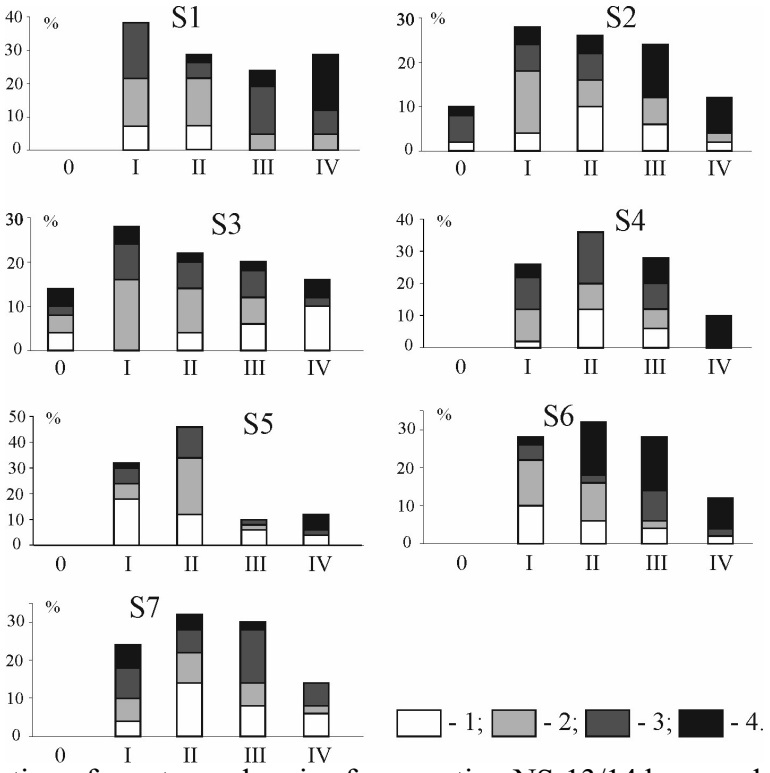

Annex 6. Distribution of quartz sand grains from section NS-13/14 by roundness and dullness. 1:glossy; 2:quater-matte; 3:half-matte; 4: matte; 0, I, II, III, IV are grades of roundness according to Khabakov (1946)

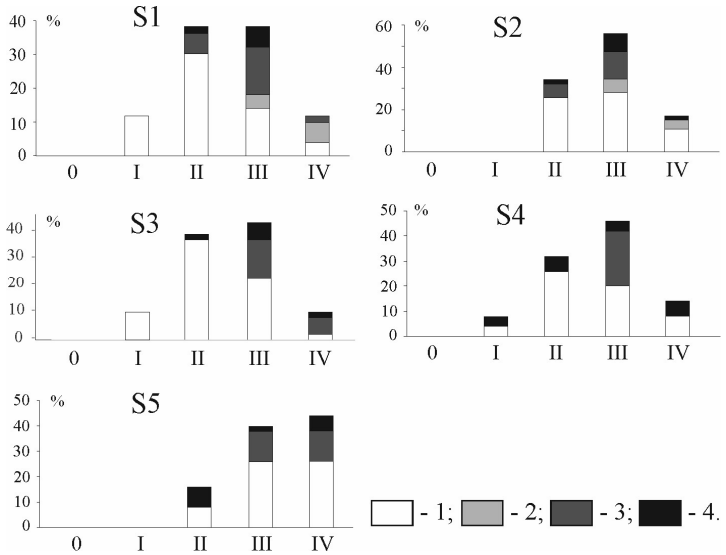

Annex 7. Distribution of quartz sand grains from section NS-20 by roundness and dullness. 1:glossy; 2:quater-matte; 3:half-matte; 4: matte; 0, I, II, III, IV are grades of roundness according to Khabakov (1946)

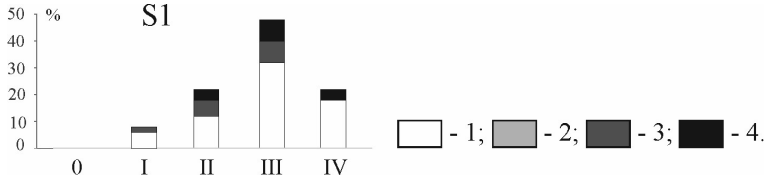

Annex 8. Distribution of quartz sand grains from section NS-22 by roundness and dullness. 1:glossy; 2:quater-matte; 3:half-matte; 4: matte; 0, I, II, III, IV are grades of roundness according to Khabakov (1946)

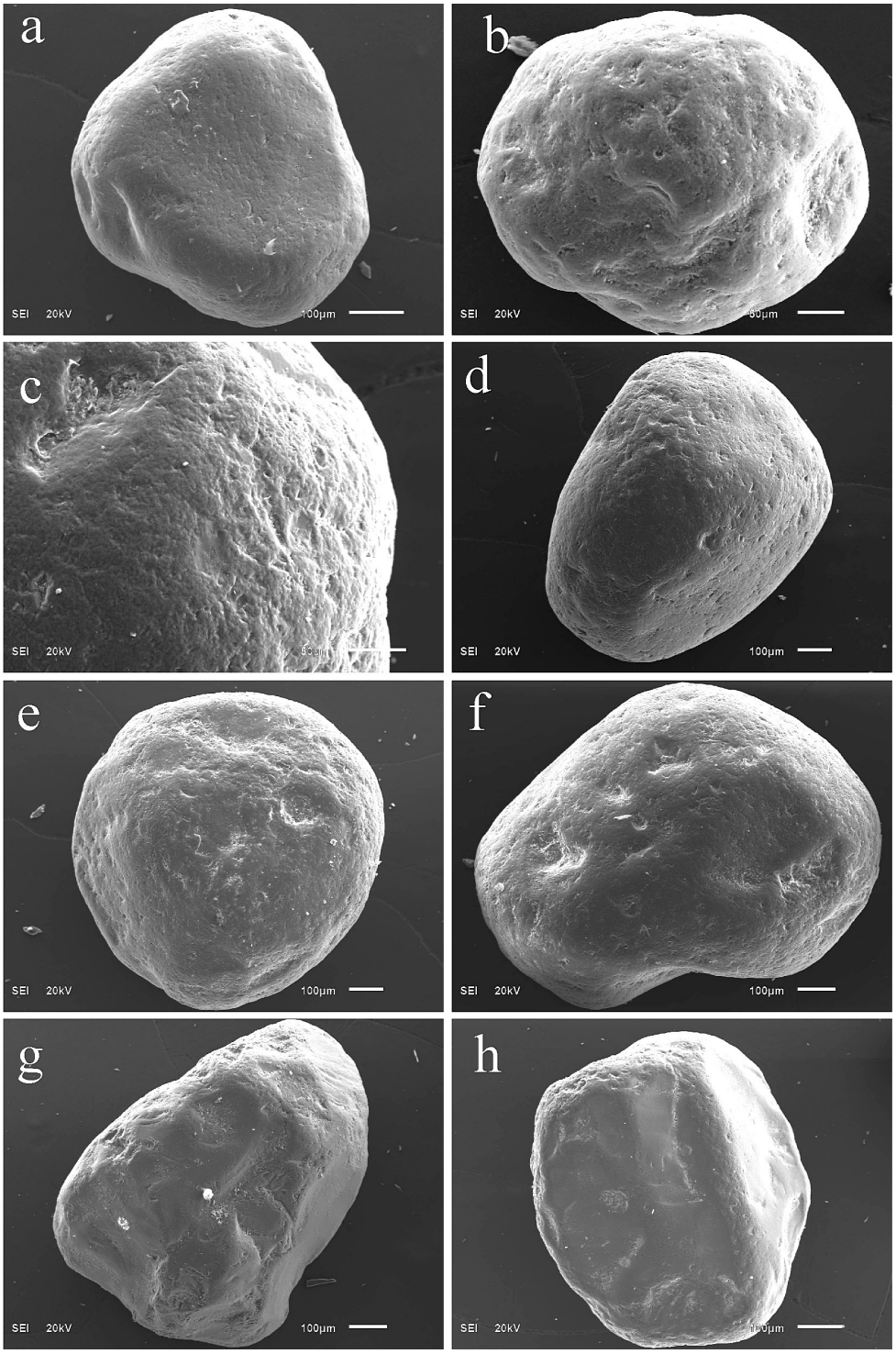

Annex 9. SEM photos of quartz grains, section NS-6.
Aeolian sediments: (a): dull grain with a micro-pitted surface and individual crescent-shaped depressions, (b): matte grain with a micro-pitted surface and traces of previous subaquatic treatment.
Floodplain sediments: (c): half-matte grain with V-shaped depressions, forming a fine-pitted surface, and with micro-pits, (d): half-matte grain with V-shaped depressions and fine-pitted.
Fluvial deposits: (e): glossy grain with a fine-pitted surface; (f): half-matte grain with a fine-pitted surface and separate V-shaped depressions; (g): glossy grain with fine-pits in the protruding parts of the grain; (h): glossy grain with presedimentation fractures, with the surface subjected to aquatic processes, as expressed by the shape of V-shaped depressions.

966

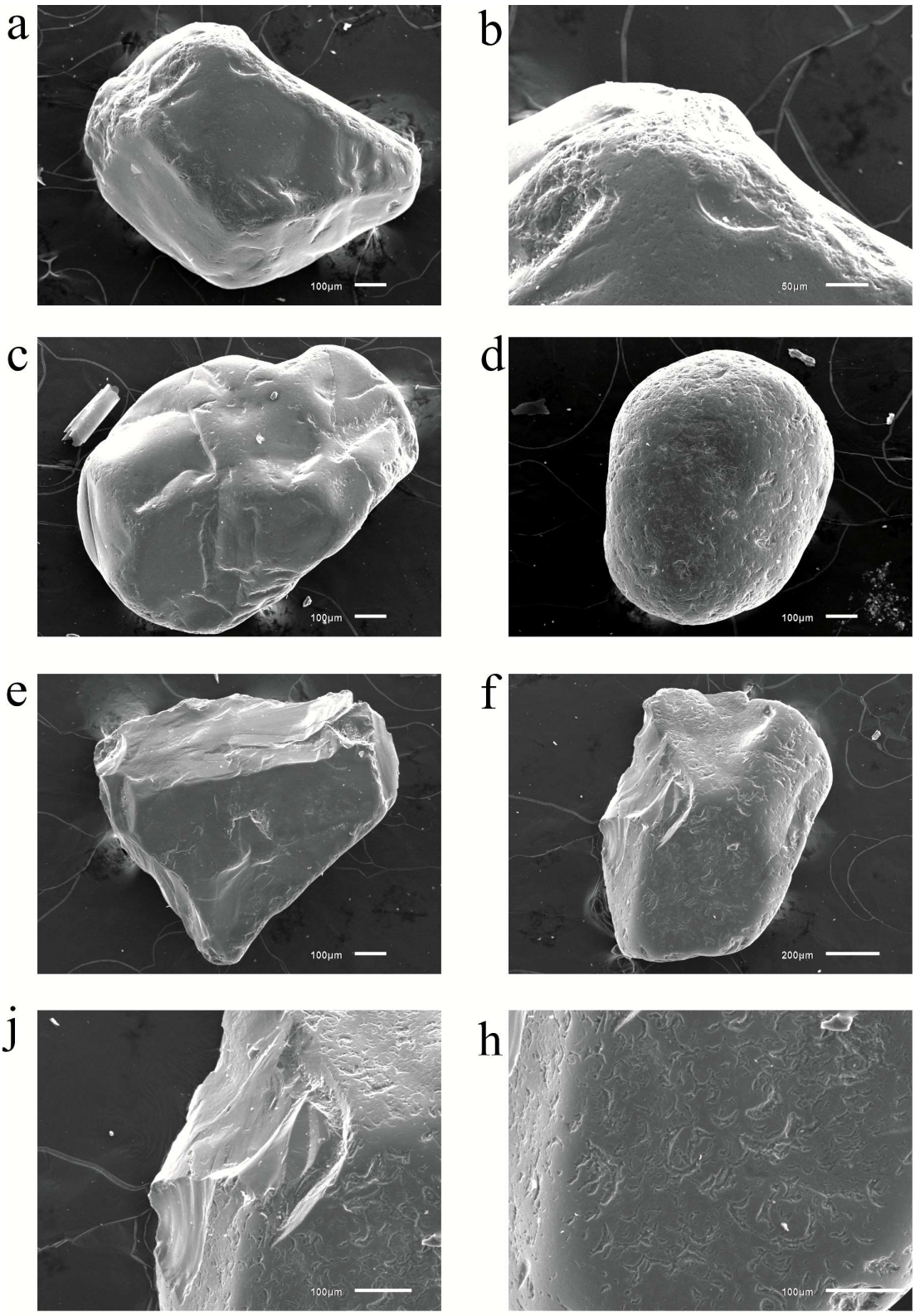

967
968 Annex 10. SEM photos of quartz grains from S7 section K-1: (a): glossy grain with a smooth
969 surface and flat faces; the faces feature crescentic pits, grain tops feature fine pits; (b): fine-pitted
970 surface of grain ‘a’; (c): glossy grain with a smooth surface and sparse fine pits; (d): half-matte
971 grain with fine-pitted surface and crescent pits; (e): glossy grain with flat faces and no evident
972 texture; (f): glossy grain with post-sedimentation conchoidal fractures and crescentic pits;
973 (j):conchoidal fracture of grain ‘e’; (h): crescentic texture of grain ‘e’.
974

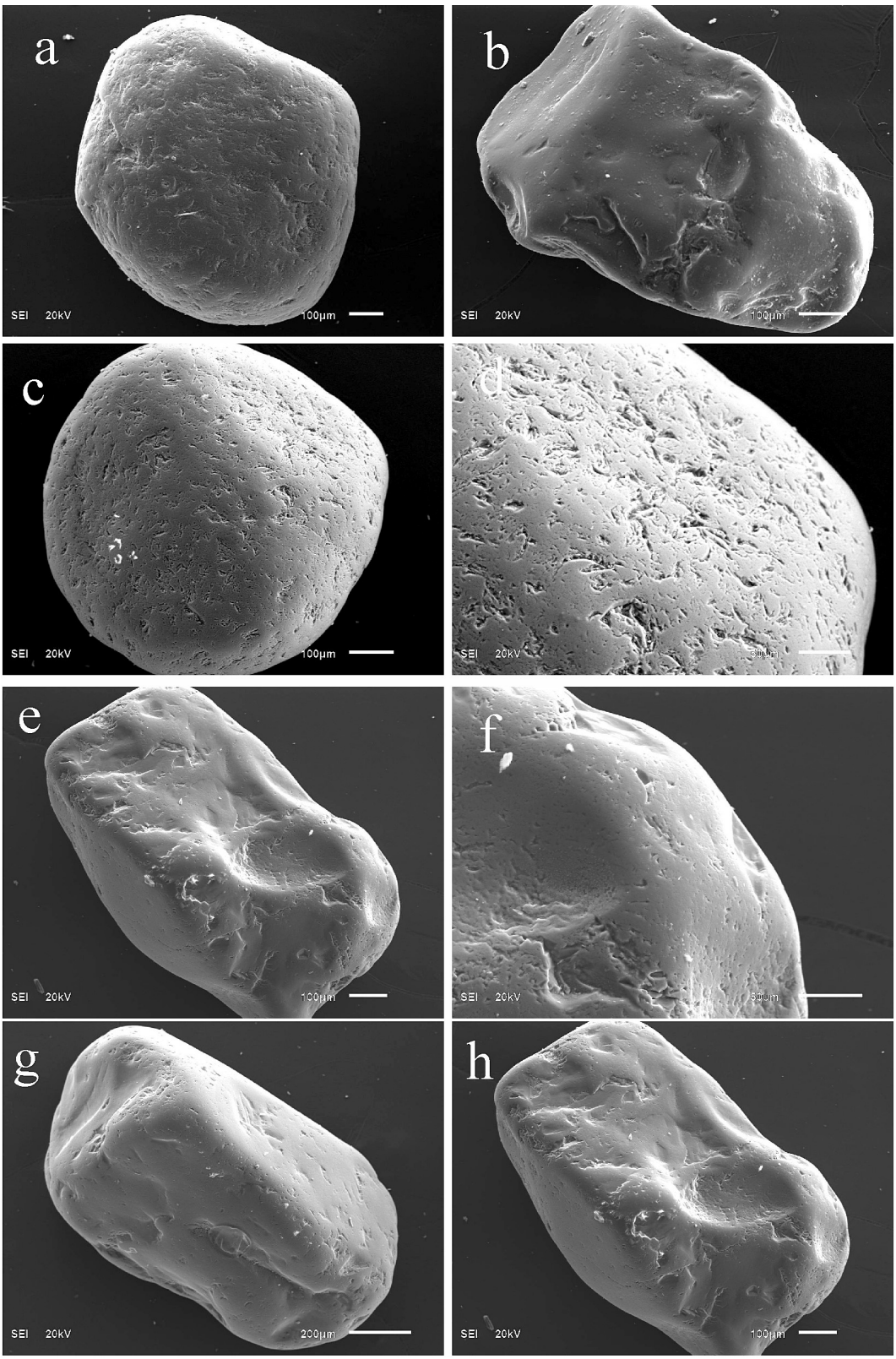

Annex 11. SEM photos of quartz grains from the section NS-13/14: (a) - glossy grain with fine-pitted and crescent and V-depressions; (b): glossy grain of irregular shape with chips and separate V-shaped recesses; (c), (d): half-matte grain with a crescentic texture and micropits; (e), (f): glossy grain with chips, V-shapes, and micro-pits on the protruding parts of the grain; (g): half-matte grain of irregular shape with a fine-pitted texture in the protruding parts of the grain; (h): glossy grain with a conchoidal fracture, V-shapes and fine-pits on the protruding parts of the grain.

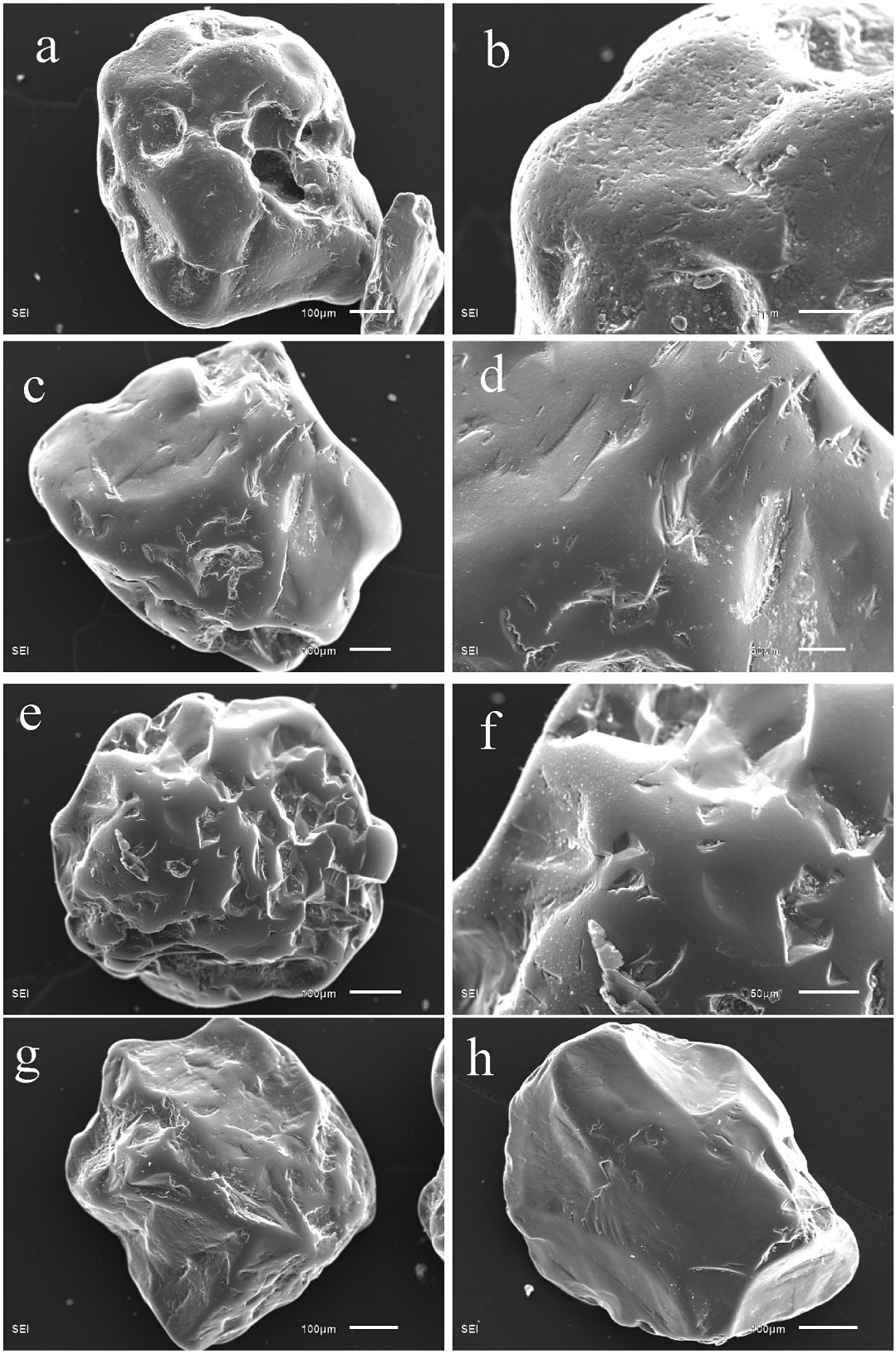

Annex 12. SEM photos of quartz grains from the section NS-20.
(a), (b): matte cavernous grain with a micro-pitted surface and individual crescentic and V-shaped percussions, (c), (d): glossy grain with a smooth surface, grooves, and individual micro-pits, (e), (f): glossy grain with deep groove and single V-shaped percussions, (g): glossy grain of irregular shape with separate V-shaped percussions and a deep-pits, (h): glossy grain with presedimental conchoidal fractures and scratches.

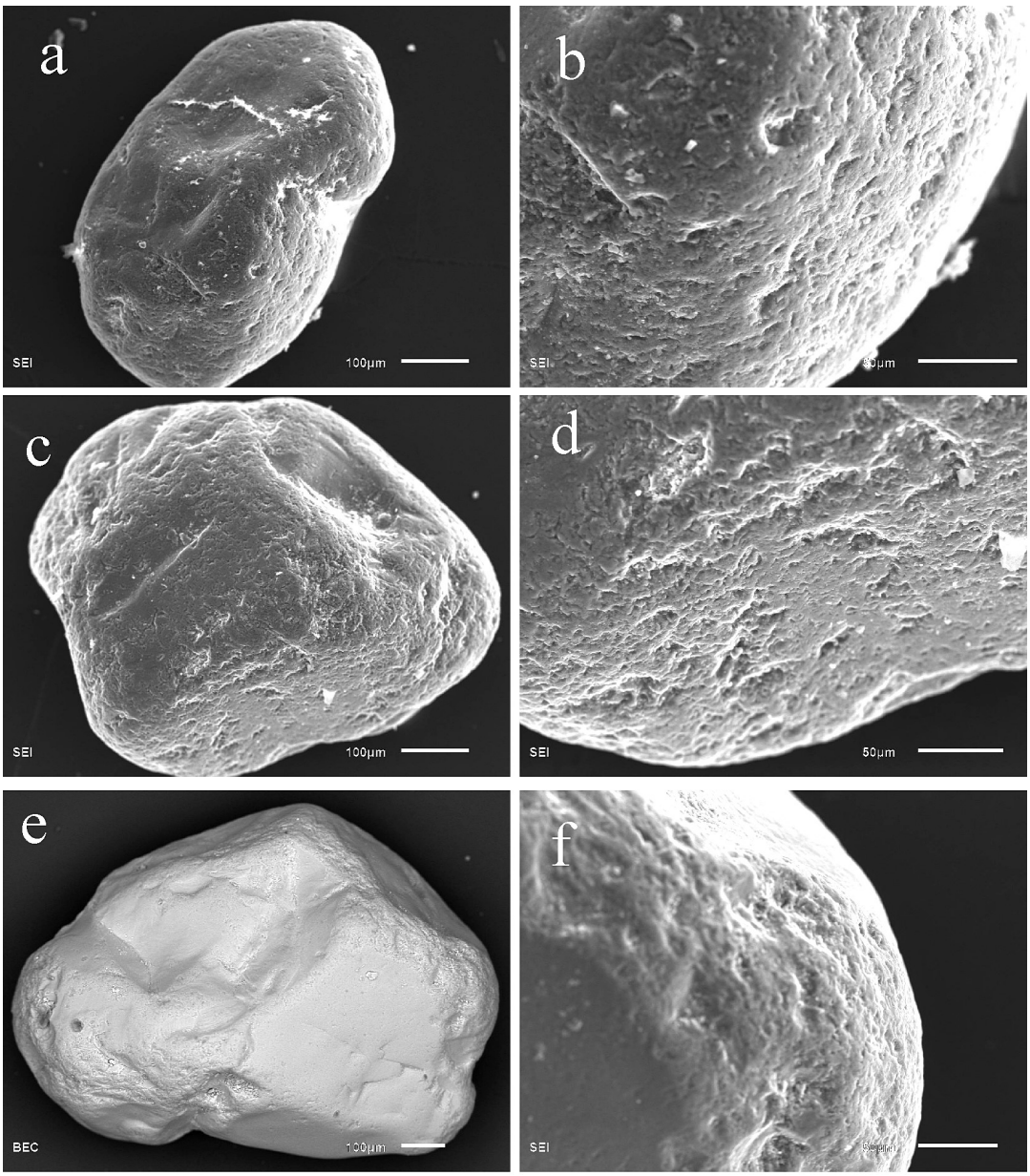

Annex 13. SEM photos of quartz grains from the section NS-22.
(a), (b): glossy grain with a fine-pitted surface, (c), (d): glossy grain with a fine-pitted surface, (e), (f): glossy grain with fine-pits on the protruding parts of the grain.